Neurochips

functionalised with cell adhesion proteins

A dissertation submitted to the
SWISS FEDERAL INSTITUTE OF TECHNOLOGY ZÜRICH

for the degree of
Doctor of Natural Sciences

presented by

Helga Maria Sorribas

Dipl. Natw. ETH
born January 12, 1973
citizen of Spain

accepted on the recommendation of

Prof. Dr. R. J. Douglas (UNI/ETHZ), examiner
Prof. Dr. P. Sonderegger (UNI-ZH), co-examiner
Dr. L. Tiefenauer (PSI), co-examiner

2001

Seite Leer /
Blank leaf

Contents

Seite Leer /
Blank leaf

Summary

During the last 20 years devices have been developed which allow extracellular stimulation and recording of neuron cells in vitro. These so called microelectrode arrays consist of either metal (gold) or indium-tin oxide electrodes or field-effect transistors on a silicon or glass chip. Extracellular recordings have been made from brain slices as well as from dissociated neuron cultures. These devices offer many advantages (long term measurements, multisite recording), however, the recorded signal intensity is not yet satisfactory. Signals measured usually ranged from 50 - 200 μV, compared to 70 mV measured with intracellular electrodes. The sealing between the neuron membrane and the electrode surface is crucial for a good signal transduction. The hypothesis of this work is that the distance between the cell membrane and the electrode surface can be reduced by culturing the neurons on neural cell adhesion proteins that are covalently bound to the surface.

Two neural cell adhesion proteins of the immunoglobulin superfamily, axonin-1 and NgCAM, have been genetically engineered. In order to achieve covalent and oriented immobilisation on glass or gold surfaces, the transmembrane and intracellular domains of the proteins were deleted and a cysteine was inserted at the C-term of the last extracellular domain near the membrane. Neurite outgrowth from dissociated chicken dorsal root ganglion neurons was observed on glass functionalised with the recombinant molecules. On Cys-NgCAM functionalised glass more neurons developed neurites than on Cys-axonin-1, and these were longer and thinner. Measurements of the cell-surface distance with fluorescence interference contrast microscopy revealed that the distance is at a minimum (37 nm) when the cells were grown on Cys-axonin-1. On RGDC substrates the distance was similar whereas on NgCAM and polylysine it was slightly larger (47 and 54 nm, respectively).

Defined neural networks in culture can be achieved by creating patterns of adhesion molecules for neurite outgrowth. In this work, a photolithographic patterning technique has been adapted to create lines and grids of RGDC and Cys-axonin-1 on glass. Two methods were used: a lift-off method was used to pattern small peptides (such as RGDC) and stable proteins. Sensitive proteins, as Cys-axonin-1, were patterned with an etching method in which the protein is protected from denaturation by a sucrose film. The adhesive patterns created in this way were shown to guide neurite outgrowth. A combination of these two patterning techniques allowed the creation of complementary patterns of two proteins on one surface.

In order to test the working hypothesis with electrophysiological recordings, a microstructured chip with a multielectrode array was fabricated by thin film technology. The electrodes

are located at the bottom of grooves (100 μm × 25 μm) in a polyimide film of 10 μm thickness. Positioning of the cells into these microgrooves was successful with a micromanipulator. However, after 1 day in culture most of the cells had moved out of the microgrooves.

In a combined experiment using the extracellular electrode for stimulation and an impaled patch electrode for recording, it could be shown that stimulation of neurons located close to the electrode is possible. The effect of the immobilised neural cell adhesion molecules on the *extracellularly recorded* signal could not be investigated during this work.

Zusammenfassung

In den letzten 20 Jahren wurden Geräte zur extrazellulären Stimulation und Ableitung von Nervenzellen in vitro entwickelt. Diese so genannten Mikroelektroden Arrays bestehen entweder aus Metall (Gold) oder Indium-Zinnoxid Elektroden oder aus Feldeffekt-Transistoren auf Silizium oder Glas. Extrazelluläre Ableitungen wurden bisher mit Hirngewebeschnitten und mit dissoziierten Nervenzellen durchgeführt. Diese Technik weist viele Vorteile auf (Langzeitmessungen, Ableitung an mehreren Stellen gleichzeitig), die gemessenen Signalstärken sind jedoch noch nicht zufriedenstellend. Die Signale liegen in der Regel zwischen 50 - 200 µV, verglichen mit den 70 mV, welche mit intrazellulären Elektroden gemessen werden. Der Abstand zwischen der Zellmembran und der Elektrodenoberfläche ist entscheidend für eine gute Signalweiterleitung. Es wurde daher die folgende Arbeitshypothese aufgestellt: der Abstand zwischen der Zellmembran und der Elektrodenoberfläche kann verkleinert werden, wenn die Nervenzellen auf neuronalen Zelladhäsionsproteinen kultiviert werden, welche kovalent auf der Oberfläche gebunden sind.

Die neuronalen Zelladhäsionsproteine Axonin-1 und NgCAM wurden gentechnisch modifiziert. Um die Proteine kovalent und gerichtet auf der Oberfläche zu binden, wurden die Transmembran- und die intrazellulären Domänen entfernt und ein Cystein wurde am C-Term der letzten extrazellulären, membrannahen Domäne eingeführt. Auf Oberflächen, welche mit den rekombinanten Proteinen funktionalisiert worden waren, konnte Neuritenwachstum beobachtet werden. Auf den Cys-NgCAM funktionalisierten Oberflächen entwickelten mehr Nervenzellen Neuriten und diese waren länger und dünner als auf Cys-axonin-1 Oberflächen. Der Abstand zwischen der Zellmembran und der Oberfläche wurde mit Fluoreszenz-Interferenz-Kontrast-Mikroskopie bestimmt. Der Abstand ist bei Nervenzellen, die auf Cys-axonin-1 gehalten werden, am geringsten (37 nm). Auf RGDC-behandelten Oberflächen war der Abstand ähnlich, wohingegen er auf Cys-NgCAM und Polylysin etwas grösser war (47 bzw. 54 nm).

Definierte neuronale Netzwerke können in vitro durch Muster von Adhäsionsproteinen entstehen, welche die Neuriten beim Auswachsen führen. In dieser Arbeit wurde eine photolithographische Methode zur Herstellung von solchen Proteinmustern weiterentwickelt. Linien und Netze aus RGDC und Axonin-1 wurden auf zwei verschiedene Arten hergestellt: Muster aus Peptiden und stabilen Proteinen können mit der Lift-off Methode hergestellt werden. Muster aus empfindlichen Proteinen, wie das Axonin-1, wurden mit der Ätzmethode hergestellt. Dabei wird das Protein von einem Zuckerfilm vor Denaturierung geschützt. Es konnte gezeigt werden dass diese Muster aus adhäsiven Proteinen die auswachsenden Neuriten führen können. Durch die Kombination der beiden Herstellungsme-

thoden konnten komplementäre Muster zweier Proteine auf einer Oberfläche hergestellt werden.

Um die Arbeitshypothese durch elektrophysiologische Messungen zu prüfen, wurden mikrostrukturierte Chips mit Multielektroden Arrays hergestellt. Die Goldelektroden befinden sich am Grund von Vertiefungen (100 μm × 25 μm) in einer 10 μm dicken Polyimidschicht. Das Positionieren der Nervenzellen in diese Vertiefungen war mit einem Manipulator erfolgreich. Die Zellen hatten die Gruben nach einem Tag jedoch wieder verlassen.

Um die Wirksamkeit der Elektroden zu überprüfen wurde eine Nervenzelle mit der extrazellulären Elektrode stimuliert und das ausgelöste Aktionspotential mit einer intrazellulären Elektrode abgeleitet. Die Auswirkung der Adhäsionsproteine auf das *extrazellulär abgeleitete* Signal konnte in dieser Arbeit nicht mehr untersucht werden.

1

Motivation

The goal of neural science is to understand the biological mechanisms that account for mental activity. Neural science seeks to understand how the neural circuits that are assembled during development permit individuals to perceive the world around them, how they recall that perception from memory, and, once recalled, how they can act on the memory of that perception. Neural science also seeks to understand the biological underpinnings of our emotional life, how emotions colour our thinking and how the regulation of emotion, thought, and action goes awry in diseases such as depression, mania, schizophrenia, and Alzheimer's disease. These are enormously complex problems, more complex than any we have confronted previously in other areas of biology (Albright et al., 2000).

The brain is the most important coordinating organ in human and animal organisms. About 10^{11} neurons in the human brain do not only control vital body functions such as respiration, blood circulation or muscle contraction, but they also provide correct processing of the external stimuli received by the sensing organs allowing us to think and to learn. Remarkable progress in understanding neuronal and synaptic signalling, plasticity, development and learning mechanisms has been made in the last years. The efforts towards an understanding of the molecular mechanisms of signal transduction have been awarded with the Nobel prize 2000 for medicine and physiology. With this knowledge a better understanding of brain functions has been possible. However, we are at the beginning of understanding and many questions concerning development, learning and consciousness remain still unsolved.

1.1 Why extracellular electrode devices?

Because of the complex 3-dimensional architecture of the brain a close examination of neural circuits with multiple intracellular electrodes in the intact brain is very difficult to per-

Table 1: Comparison of different types of neuron recording systems[a,b]

Electrode Type	Noninvasive	Stimulation through electrode	Signal size or S/N-ratio	Sealing to substrate	Subthreshold recording	Long term recording	Multisite recording	Dendrite recording	Surface coating
Intracellular	N	Y	100%	N	Y	N	Y	Y	
Voltage sensitive dyes	N	N	10:1	N	N	N	Y	Y	
FET[c]	Y	Y	25%	Y	Y	Y	P	P	polylysine
Diving board[d]	Y	P	100:1	Y	P	Y	N	N	
Multielectrode array[e]	Y	Y	5:1	Y	P	Y	Y	P	flamed polysiloxane
Multielectrode array[f]	Y	Y	4:1	Y	P	Y	Y	Y	ConA
Multielectrode array[g]	Y	Y	500:1	Y	P	Y	Y	P	ConA
Multielectrode array[h]	Y	N	30:1	Y	P	Y	Y	P	laminin, NGF
Multielectrode array[i]	Y	Y	70:1	Y	P	Y	Y	N	polylysine, laminin

a. adapted from Curtis et al., 1994
b. N: No, or not applicable; P: possibility; Y: yes
c. Fromherz et al., 1991; invertebrate neuron
d. Regehr et al., 1988; invertebrate neuron
e. Gross and Schwalm, 1994
f. Wilson et al., 1994
g. Breckenridge et al., 1995; invertebrate neuron
h. Bove et al., 1997
i. Maher et al., 1999

form. Neural processing, plasticity and learning cannot be thoroughly investigated. Advances in culturing techniques have enabled to culture brain tissue slices as well as dissociated neurons on microstructured surfaces containing arrays of extracellular electrodes for stimulation and recording. These so called microelectrode arrays (MEA) allow to perform experiments on signal transduction and processing in vitro.

An important criterion when designing neural networks is the interfacing method (a comparison of different types of recording systems is given in Table 1). Widely used for the study of neural activity is intracellular recording. This method is very sensitive and good signal-to-noise ratios (S/N-ratio) are obtained. However, intracellular electrodes kill the cell after a few hours of recording, and simultaneous measurements at more than two positions are very difficult to perform. Potential-sensitive dyes offer the advantage of sampling over large areas of tissue, however the dyes are often cytotoxic and S/N-ratios are poor. Reports of measurements on single cells with extracellular microelectrodes have been published quite some time ago (Krnjevic and Miledi, 1958), but only with the advent of the integrated circuit technology the electrodes size could be reduced to cellular dimensions. The advantages of extracellular electrode arrays for the study of neuronal network activity are considerable (Breckenridge et al., 1995):

- The technique is non-invasive and thus it is possible to record from neurons over extended periods of time. For example, spinal-cord neurons have been cultured for up to one year on microelectrode arrays (Gross et al., 1995).

- It is possible to record from more than one cell in a network simultaneously over long periods of time (Jimbo et al., 1993; Gross et al., 1995).

- Because of the very small size of the electrodes the neuron can make contact with more than one electrode so that the activity in the cell body, axon and dendrites can be sampled simultaneously (Wilson et al., 1994).

- Predetermined networks of neurons can be constructed patterning the substrate topographically or chemically (see chapter 2).

- The in vitro environment allows highly reproducible pharmacological manipulations with no interference from other organs, allowing applications in neurotoxicology, drug development and biosensors (Gross et al., 1997a).

Two types of extracellular electrodes have been established: The low impedance metal electrodes such as (platinised) gold or the optically transparent indium-tin oxide on the one hand and the field effect transistor devices (FET) on the other hand. Planar multielectrode arrays have been used to study signal propagation and synchronisation events in brain tissue slices (Kamioka et al., 1997; Duport et al., 1999; Oka et al., 1999) and in random networks of dissociated neurons (Maeda et al., 1995; Kamioka et al., 1996). Other groups have recognised the potential use of neural networks as sensor devices for drugs and toxins (Gross et

al., 1997b; Harsch et al., 1997). Applications for retina-based visual prostheses are also being discussed (Grumet et al., 2000).

Single cell measurements have been reported mostly for invertebrate neurons. These neurons are larger in size and are therefore considered to make better sealing to the electrode. Indeed, it was found, that signals in the mV regime can be recorded from such cells (Regehr et al., 1989; Breckenridge et al., 1995). Earlier, Regehr and coworkers (Regehr et al., 1988) had stimulated and recorded from an invertebrate neuron with an electrode sealed from the top. Reports on single, vertebrate neuron recordings are rare. Maher et al. (1999) could place a neuron in an inverted pyramidal groove with an electrode at the bottom. They recorded spontaneous activity as well as stimulated activity and the recorded signals ranged from 50 to 200 µV. Single cell measurements have also been reported with FET devices (Fromherz et al., 1991; Offenhäusser et al., 1997). These signals resemble more the shape of the action potential and not first or second order time derivatives thereof as is the case with extracellular metal electrodes, indicating that the sealing of the cell membrane to the surface is better on silicon oxide than on metal surfaces (Grattarola and Martinoia, 1993).

1.2   Signal recording with extracellular electrodes

The ideal recording electrode should record only from a small group of cells and have a geometry that maximises signal pick-up from impinging action potentials. Lind et al. (1991) showed with finite-element analysis that the electrode potential of a planar electrode is increased more than seven times if the cell and the electrode are confined in a narrow groove or in a cubic pit of 25 µm depth. For a good S/N-ratio the electrodes should have the lowest possible impedance. Impedance reduction is achieved by increasing the surface area with platinum black deposition (Breckenridge et al., 1995) or roughening the surface with etching reagents (Kovacs, 1994). The ideal stimulating electrode should have zero crosstalk with other electrodes. That is the case if the electrodes are 100 µm ore more distant (Breckenridge et al., 1995).

The recorded extracellular signal is a measure of the ionic current rather than the membrane potential (V) per se (Connolly et al., 1990). A simple approximation is that the extracellular current is proportional to the change in the membrane voltage dV/dt. The magnitude and temporal characteristics of a recorded action potential depend on local conditions (Curtis et al., 1994). Fig. 1 shows the equivalent circuit model of a metal electrode. The top part of the circuit represents the neuron cell compartment with its membrane capacitance, resistance and voltage. The bottom part shows the electrode properties (capacitance and resistance). The junction between the cell and the electrode is represented by the sealing and the spreading resistance (see also Fig. 2). The seal resistance R_{seal} models the resistive component of
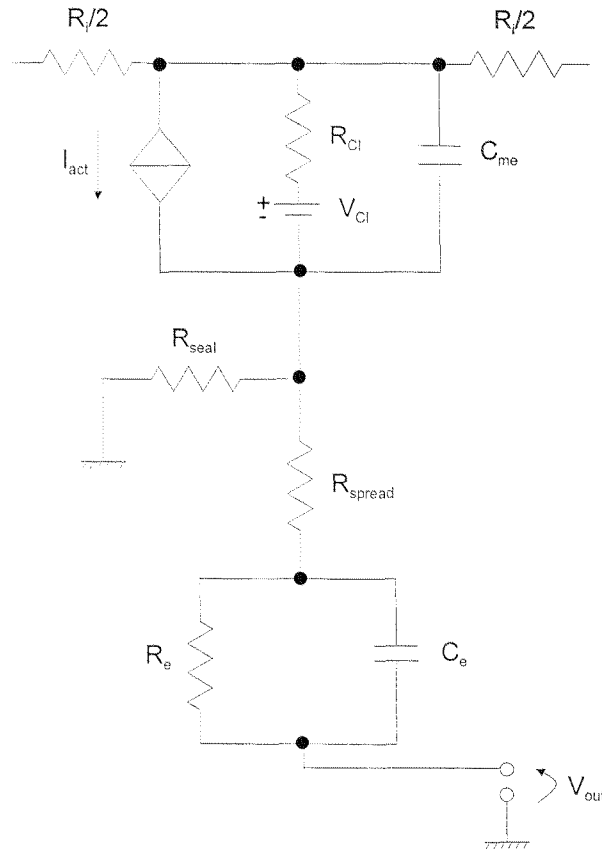
Figure 1: Equivalent circuit model of the cell-electrode contact

Circuit between a neuron membrane patch and a planar noble metal microelectrode. The top part of the circuit represents the cell, the bottom part represents the electrode. R_i: cytoplasmic resistance connecting two adjacent compartments; R_{Cl} and V_{Cl}: chloride resistance and equilibrium potential; I_{act}: sum of Na, K and Ca-currents; C_{me}: cell membrane-electrolyte capacitance (consisting of membrane capacitance C_m, Helmholtz capacitance C_h and diffuse layer capacitance C_d); R_{seal}: sealing resistance between cell and microelectrode; R_{spread}: spreading resistance; R_e and C_e: resistance and capacitance of electrode-electrolyte interface. The sealing impedance is represented by the RC coupling circuit consisting of C_{me}, R_{seal}, and R_{spread}. Adapted from Grattarola and Massobrio, 1998.

the thin layer of solution between the cell membrane and the microelectrode and is affected by the distance d between the cell membrane and the electrode surface through the relation

$$R_{seal} = \frac{\rho_e}{4\pi d}$$

where ρ_e is the medium resistivity (typically 0.7 Ωm for a loose sealing, 1 – 5 Ωm for a tight seal; Grattarola et al., 1991). A reasonable value of R_{seal} in the range of 1 to 5 MΩ is obtained by assuming ρ_e= 0.7 Ωm and 10 nm < d < 50 nm (Grattarola et al., 1991). Using the SPICE

simulation program the group of Grattarola could show that the measured extracellular voltage (V_{out}) is increased 8-fold if the distance d is reduced from 50 to 10 nm (Grattarola et al., 1991). Additionally, reduction of the spreading resistance R_{spread} from 500 kΩ to 5 kΩ was also shown to improve the signal measured, however with much less efficacy (Grattarola et al., 1991). The spreading resistance R_{spread} describes the net resistance encountered by a current spreading out from an electrode into a conductive solution. It is determined by the geometric surface area of the electrode (Kovacs, 1994). Similar results are obtained with
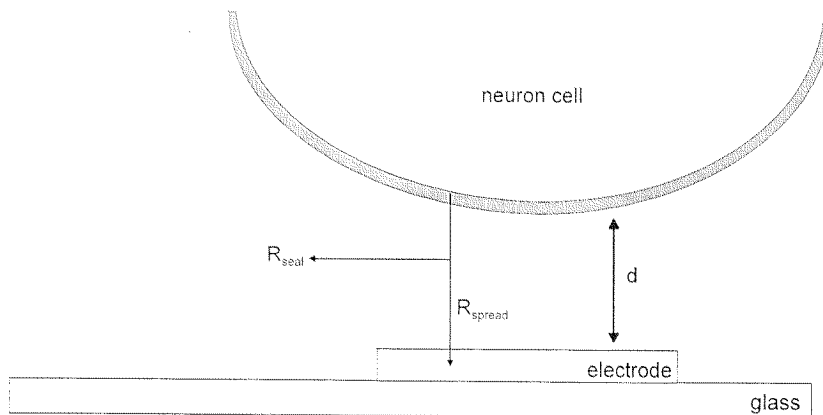
Figure 2: Schematic drawing of a neuron cell on an electrode

The signal sensed by the extracellular metal electrode depends on the sealing and spreading resistances (R_{seal} and R_{spread}, respectively). A high sealing resistance is obtained by reduction of the cell-electrode distance d.

the extracellular electrodes described by Breckenridge et al. (1995). They found that the relative impedances of the across-the-electrode (R_{spread}) and the electrode-to-earth paths (R_{seal}) determined both the magnitude and shape of the recorded signal. Very good sealing with a sealing resistance exceeding 1 MΩ led to relatively large signals on the order of 1 mV when action potentials occurred in large invertebrate neurons. The *shape* of the signal changed with the effectiveness of the cell sealing over the underlaying electrode. The recorded signal strength increases proportionately to the increase in seal impedance (Curtis et al., 1994; Breckenridge et al., 1995). Additionally, as the seal impedance increases, the signal shape comes to approximate the intracellularly recorded potential changes. Measurements on cells with low sealing resistances resemble the first or second order time derivative of the intracellularly recorded signal (Grattarola and Martinoia, 1993; Curtis et al., 1994). It is still uncertain whether subthreshold events and slowly changing potentials can be detected by this type of electrode (Curtis et al., 1994; Denyer et al., 1997). The S/N-ratios of the recording are improved by locating the electrode in a relatively deep groove (Lind et

al., 1991). The reason for this is probably that the ionic transients accompanying the action potential are not dissipated by diffusion to extracellular space as rapidly as they would be in planar arrays. Wilson et al. (1994) laid a sheet of ganglion capsule over a leech neuron to provide additional contact surface thereby increasing the S/N-ratio.

1.3   Aim of the project

The major aim of this project was to evaluate if neural cell adhesion proteins used as substrate for culturing dissociated neurons could reduce the cell-surface distance and thus increase the S/N-ratio of the recorded signals. The project was divided in different parts:

- The domain interaction models of the neural cell adhesion proteins axonin-1 and NgCAM suggest, that these proteins could probably induce a tight cell-surface contact. The proteins were genetically engineered in order to obtain a covalent and oriented immobilisation on glass and gold.

- Glass surfaces were functionalised with these recombinant proteins and with other cell adhesion molecules and the effects on outgrowing dissociated dorsal root ganglion neurons were investigated.

- An extracellular electrode array for stimulation and recording of single neurons was fabricated. The electrodes are located in grooves. One neuron cell would fit into one groove allowing selective stimulation and recording of single cells.

- Different methods for positioning neurons into the grooves were tested.

- Methods for a localised immobilisation of different proteins on the same surface were investigated.

- Electrophysiological experiments with neurons cultured on the electrode array were planned for a validation of the chip and the chip-interface.

- The effect of the immobilised adhesion proteins on the S/N-ratio of the extracellularly recorded signals were planned to be tested with electrophysiological recordings.

Seite Leer /
Blank leaf

2

Chip Fabrication and Protein Patterning

2.1 Introduction

2.1.1 Chemical and topographic nerve cell guidance

In order to construct living neural networks in vitro, it is important to consider in which form guiding signals are normally presented to the growing nerve cells in vivo. During development of nerve cell connections the leading tip of the growth cone senses its surroundings and then decides which way to follow. Guidance cues can be the surface chemistry and the shape of the tissue and extracellular matrix surrounding the growth cone, diffusion gradients consisting of sources of diffusible morphogens, specific signalling molecules and endogenous electric-field gradients. These chemical guidance cues can be attractive or repulsive (see chapter 3). Attempts to control nerve cell adhesion and growth by modifying the surface chemistry of the cell culture substrates date back to the work of Letourneau (1975). He used a transmission electron microscope grid to mask off areas of substrate coated with polystyrene, collagen, polyornithine and the less adhesive palladium. Other groups have patterned natural adhesion molecules derived from the extracellular matrix (Hammarback et al., 1985; Lom et al., 1993; Fromherz and Schaden, 1994), fragments of adhesion proteins (Massia and Hubbell, 1990; Matsuzawa et al., 1996), growth factors (Gundersen, 1985) and membrane fragments (Vielmetter et al., 1990). Patterned substrates have been fabricated using selective UV denaturation (Hammarback et al., 1985), photolithographically directed adsorption of molecules to the surface (Kleinfeld et al., 1988; Lom et al., 1993), stamping (Branch et al., 1998) and ink-jet printing (Klebe, 1988).

Topographic guidance was discovered in 1936 by Weiss (Weiss, 1945) who showed that neurons in culture prefer to spread along lineated structures such as fine fibres. With the

advent of microfabrication techniques it has become possible to study this phenomenon systematically (for a review see Curtis and Wilkinson, 1997; Flemming et al., 1999). Elevations as small as 40 nm can be sensed by certain cells (e. g. a macrophage-like cell line; Wojciak-Stothard et al., 1996). But different cell types respond differently to topography. Rat dorsal root ganglia neurons, for example did not align to 12–100 μm pitch grooves which were less than 1 μm deep. The proportion of aligned neurites increased with groove depth. Maximum neurite alignment was seen with 6 μm deep, 25 μm wide grooves (Britland et al., 1996). The mechanism of topography recognition is not fully clear. Do the cells just sense discontinuities in the substrate as Curtis and Wilkinson (1997) propose? Or does the structuring of the substrate alter the surface chemistry which is recognised by the cells? Britland et al. (1996) combined a chemical cue (laminin) superimposed orthogonally over a topographic one. When the grooves were 500 nm deep or less, the cells responded mainly to the chemical cue. On deeper grooves the topographic cue over-rode the chemical one and at 6 μm depth the topographic effect oriented about 80% of the cells and the chemical one 7%. If the chemical and the topographic cue were oriented in parallel a synergistic effect was observed at groove depths of 100 nm and more and 25 μm groove width. The authors conclude that chemical and topographic guidance cues can interact synergistically and hierarchically to steer nerve cell growth.

2.1.2   Protein patterning techniques

Chemically defined surfaces can be used to directly examine substrate-guided neurite outgrowth in vitro, but also for the production of miniaturised biosensor devices. Several techniques for patterning biomolecules onto surfaces in micrometer scale have been developed in the last years (reviewed in Blawas and Reichert, 1998). Protein patterning is a localised form of protein immobilisation. The simplest method for immobilising proteins on surfaces is physical adsorption. A more stable means of protein immobilisation is to covalently link a protein to a surface via a chemical bond between molecules on the surface and the protein. Protein immobilisation with similar stability can be achieved using high-affinity ligand pairs such as avidin-biotin, protein G and protein A.

In 1978 MacAlear and Wehrung used photoresist technology from the semiconductor industry to create patterns on an underlying compressed protein layer (MacAlear and Wehrung, 1978). The technique has been further adapted for patterning of proteins (Fig. 5A). A photoresist is spin coated on a (glass) surface, exposed through a mask and developed, resulting in a resist pattern on the surface. Molecules with different terminal groups, most often silanes which withstand the harsh solvents required to remove the photoresist, are now patterned on the surface. The glass slide is immersed in a chemically activated silane solution resulting in a derivatisation of the surface. The resist is then removed and a second activated silane can bind to the now exposed surface areas resulting in a complementary pattern of two silanes on one surface. Initially, patterns of silanes with different

hydrophilicity were created to guide neurite outgrowth (Kleinfeld et al., 1988). An amino-terminated silane promoted cell attachment, whereas an alkyl-terminated silane would suppress cell attachment, leading to guided neurite outgrowth. Other groups have used patterns of two different silanes as surfaces for the selective adsorption of outgrowth promoting proteins (Lom et al., 1993). A different approach was described by Flounders and colleagues for patterning surfaces with antibodies (Flounders et al., 1997). First the antibody was immobilised on the entire surface and protected by a sucrose layer during the further process steps. A photoresist layer was then patterned on the protein film serving as a mask in the subsequent plasma etching step. The exposed protein molecules were removed in this etching step. The protein patterns protected by the photoresist appeared after resist removal. The immobilised antibody retained its function as was shown by binding fluorescence-labelled antibodies. Nicolau et al. (1999) exposed a photoresist to UV light in order to create carboxylic-rich areas on the resist. The patterned resist surfaces where then further functionalised with peptides specific for cell attachment.

Direct patterning with light has been developed by several groups. Some make use of photochemically active molecules to create functional groups on surfaces which can be further derivatised with biomolecules (reviewed in Sigrist et al., 1995). Other groups have used UV-light to inactivate or to remove immobilised biomolecules (Hammarback et al., 1985; Matsuzawa et al., 1996; Vaidya et al., 1998).

A popular method for patterning proteins is microcontact printing, also called soft lithography. A structured polymer stamp is cast from a microstructured silicon wafer and used to transfer molecules from solution to a solid support (Mrksich and Whitesides, 1995; Kane et al., 1999 for a recent review). The technique was initially developed to transfer self-assembled monolayers from the stamp to a (gold) surface. Recently, it has been applied to stamp polylysine on glass slides pretreated with a silane and a crosslinker reagent for covalent binding of the polylysine to the surface (Branch et al., 1998). If the microstructured polymer is sealed with a flat surface on the top a network of channels is obtained. These can be used as microfluidic networks to pattern multiple molecules or even cells on a surface (Delamarche et al., 1997; Martinoia et al., 1999; Chiu et al., 2000).

2.2 Methods

All chips were produced from 5 inch glass wafers (alkali-free glass type SD2; Hoya, Germany) cleaned with a 8 min CAROs etch (H_2SO_4:H_2O_2 = 2:1 v/v) at 95 °C and a 1 min HF-dip (HF:H_2O=1:10 v/v). The fabrication processes were done in a class-10 clean room.

2.2.1   Gold chip production

An titanium adhesion layer (15 nm) was evaporated on cleaned glass wafers followed by evaporation of a 40 nm thick gold layer with electron-gun-evaporation (BAK600, Balzers). The wafer was coated with a protective photoresist film and cut into pieces of (1×1) cm with a wafer saw. Glass chips which were only half coated with gold were produced by photolithography and lift-off of whole wafers. A positive photoresist was exposed through a mask with 1 cm wide stripes. Films of titanium and gold were evaporated as described above. The photoresist was removed with resist remover resulting in alternating 1 cm wide stripes of gold and glass. To obtain (1×1) cm half glass/half gold chips the stripes were sawed in the middle.

2.2.2   Fabrication of microstructured chips

For the chip production standard thin-film technology was used. A set of three masks was designed to form the electrodes and conducting lines (Fig. 3, mask 1), the insulating layer (mask 2) and the groove defining polyimide layer (mask 3), respectively. The gold micro-electrode array was produced by lift-off technique (Fig. 4): The mask 1 was used to structure a positive photoresist on which a thin titanium adhesion layer (15 nm) and a gold film (40 nm) were evaporated (BAK600, Balzers; Fig. 4, 1 – 3). The gold electrode array resulting from photoresist removing was insulated by a 200 nm SiO_2 passivation layer which was deposited by evaporation (Fig. 4, 4). Using mask 2 100 µm × 25 µm wide grooves were opened in a layer of resist above the oxide. This layer was then used as an etch mask during oxide etching in NH_3-buffered HF, thus transferring the grooves to the insulating layer and exposing the electrodes (Fig. 4, 5). For the definition of the microgrooves a photosensitive polyimide (Probimide P-7020, OCG Microelectronic Materials AG, Switzerland) was used. Due to its dielectric properties this layer served as second insulating layer. The spin-coating conditions envisaged a final layer thickness of 10–15 µm. After light exposure (mercury lamp 350–450 nm) through mask 3 and development the polyimide was cured at 350 °C in a N_2-ventilated oven using the temperature profile recommended by the manufacturer (Fig. 4, 6 and 7).

For the electrophysiological experiments described in chapter 5 chips with a silicon nitride layer were used. The fabrication steps were identical to the above described. Instead of a polyimide film, a 400 nm thick Si_3N_4 passivation layer was sputtered on the wafer (Leybold Z2600, Germany). A positive photoresist was exposed through a dark-field copy of the polyimide mask (bright-field mask). The photoresist patterns served as a mask during etching of the silicon nitride layer with a reactive-ion-etch ($O_2:CHF_3 = 3:40$ v/v). The micro-structured wafers were then coated with a photoresist layer to protect the surface from dust and sawed into (1×1) cm pieces.

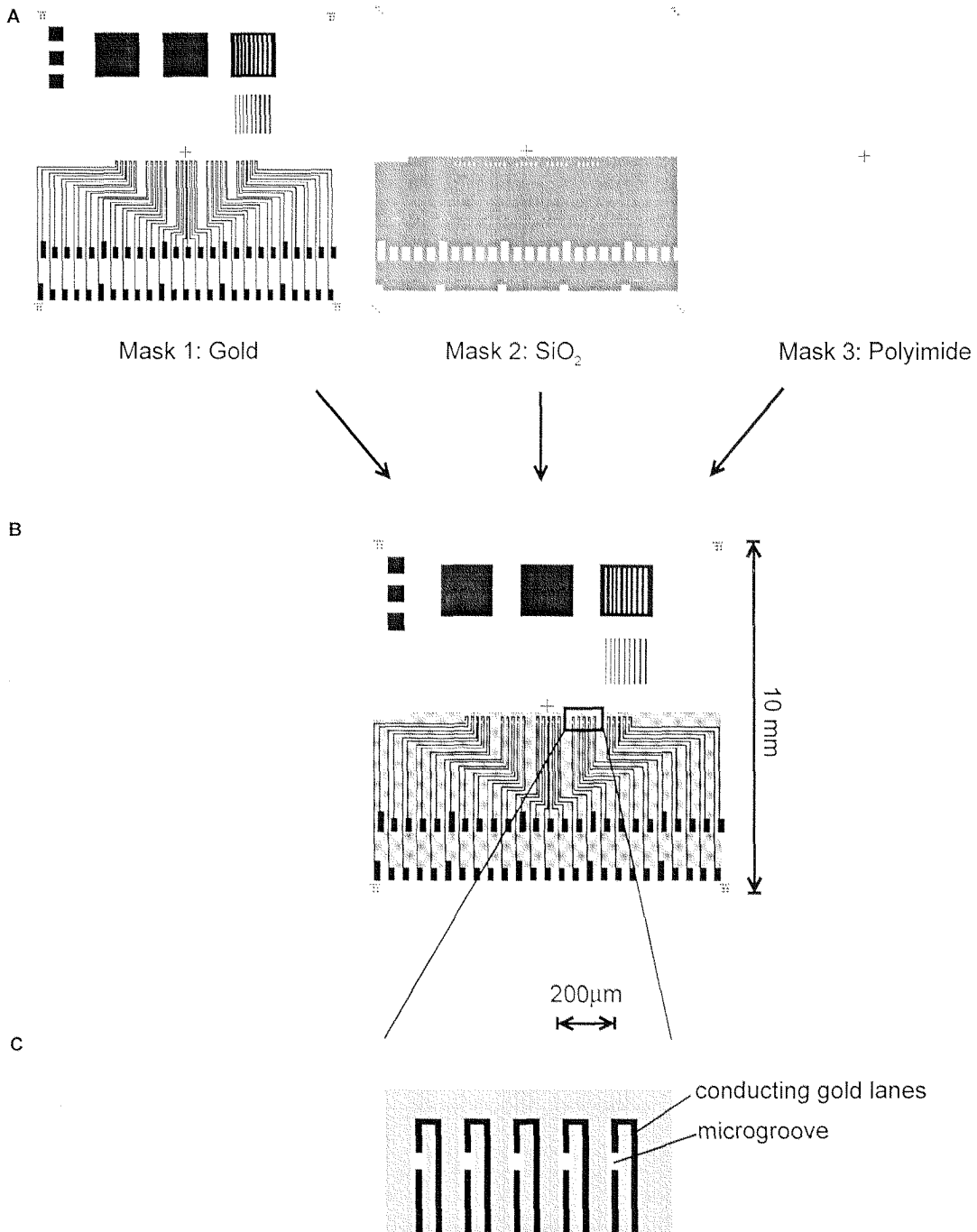**Figure 3: Mask design for the production of the microstructured chips**

Three photolithographic masks (A) were designed for the structuring of the conducting gold lines (mask 1), the insulating silicon oxide layer (mask 2) and the polyimide (mask 3) resulting in a micro-structured chip (B). The microgrooves with the electrodes for neuron cell stimulation and recording are located in the centre region of the chip (C).

photoresist structuring (1)

gold evaporation (2)

lift-off (3)

SiO$_2$ deposition (4)

buffered etch (5)

polyimide spinning (6)

light exposure and development (7)
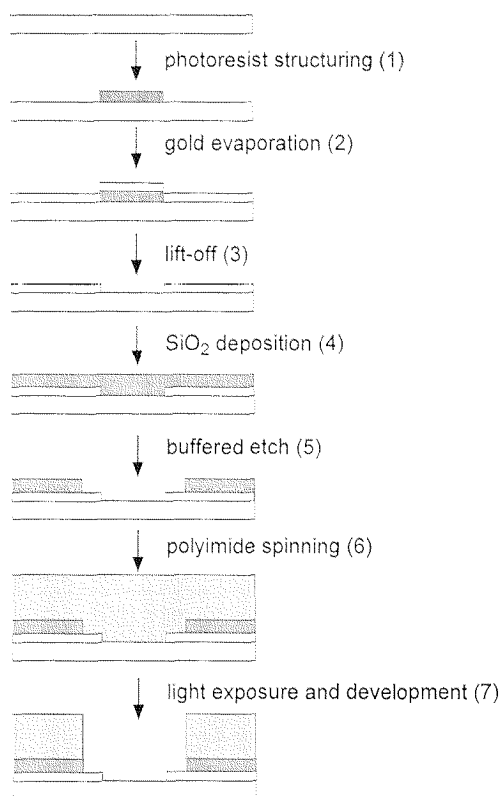
Figure 4: Fabrication of microstructures

A structured photoresist served to form the gold electrode tracks by lift-off (1-3). An insulating silicon oxide layer was deposited and structured by buffered HF-etch (4,5). Finally a photosensitive polyimide was spun on the wafer (6) and structured by light (7). Alternatively a silicon nitride layer was sputtered on the surface and structured by photolithography and reactive ion etching.

2.2.3 Chip handling

The chips were contacted via wire bonds to a custom designed print board (Fig. 23). The chip was glued onto the print board with a two-component glue (Epotek377, Epoxy Technology Inc., USA) and bonded with an Al-wire (25 µm) using a hand-bonder (MEI 1204W, Marpet Enterprise Inc., USA). Due to space limitations on the printed circuit board the bottom row of electrodes (25 contacts) were contacted via 4 pads. Three pads were connected with 5 electrodes each and the forth with 10 electrodes (Fig. 6D) The microelectrodes of the upper row were each connected to a separate pad. The bond wires and the printed cir-

cuit board were embedded with a silicon elastomer (PDMS; Sylgard 194, Dow Corning) to protect the wires from mechanical and chemical (buffer, cell media) stress. A glass ring (6 mm inner diameter, 8 mm height; Bellcon Glass, Inotech, Switzerland) was placed on the chip to protect it from the PDMS. This glass ring served as solution container during immobilisation and as cell culturing chamber. The PDMS was cured in an oven at 100 °C during 15 min. Wires were soldered on the contacts on the outside of the board. They served for the connection to a pulse generator during the electrophysiological experiments (chapter 5). Between each new culturing experiment the bonded chips were rinsed with a water jet to remove impurities. Then a 10% sodiumdodecylsulfat solution was applied on the chip for 15 min and rinsed extensively with H_2O^1. The chip surface was finally etched (H_2SO_4:H_2O_2 = 1:3 v/v) for 1 min followed by rinsing in H_2O.

2.2.4 Chip characterisation

The functionality of the gold electrodes and the contacts was electrochemically tested with cyclic voltammetry. A drop of a 1 mM N-(ferrocenylmethyl)-6-aminocaproic acid (Padeste et al., 2000) solution in phosphate buffer was positioned on the chip above the electrodes, and a reference and a counter electrode were immersed in the same drop. The extracellular electrode was connected as a working electrode to the low current module of a potentiostat for electrochemistry (PGSTAT20, Ecochemie, Holland). A potential gradient was applied and the corresponding current was measured. One or more electrodes were addressed and the response measured (Fig. 7). To test electrode crosstalk, one electrode was connected to a bipotentiostat module to hold the potential at a given voltage. A second microelectrode was the working electrode on which redox-reaction was monitored.

2.2.5 Photolithographic patterning of proteins

Two methods were used to generate patterns of proteins on glass surfaces: the lift-off and the etching method (Fig. 5A, B). The critical step in photolithographic patterning is the removing of the resist with acetone. Immobilised proteins can be denatured by this solvent. The lift-off method was thus used to immobilise small peptides (RGDC) and stable proteins such as antibodies or streptavidin. The more labile proteins Cys-axonin-1 and Cys-NgCAM were patterned using the etching method, in which the immobilised protein layer is protected by a sucrose film. Combining the two methods a second molecule can be immobilised and complementary patterns of proteins can be created (Fig. 5C).

In the lift-off method (Fig. 5A) glass chips were cleaned with acetone and iso-propanol. A positive photoresist (S-1813, Shipley) was spin-coated on the chips (3000 rpm, 30 s) and

---

1. H_2O is used throughout the text for ion exchange purified water (18.2 MΩcm, Milli-Q, Millipore, USA)

soft-baked on a hotplate during 1 min at 90 °C. The chips were aligned with the mask using a mask-aligner (MA6, Karl Suess, München). The resist was irradiated (350–450 nm mercury lamp) during 5 s and developed (10–15 s; MF-319, Shipley). Development was stopped by soaking in water for a few seconds. Immobilisation of proteins was done as described in 3.2.1, using isooctaneisooctane as the solvent in the silanisation procedure instead of toluene, which would attack the photoresist. The resist was removed by sonication in acetone (2 min).
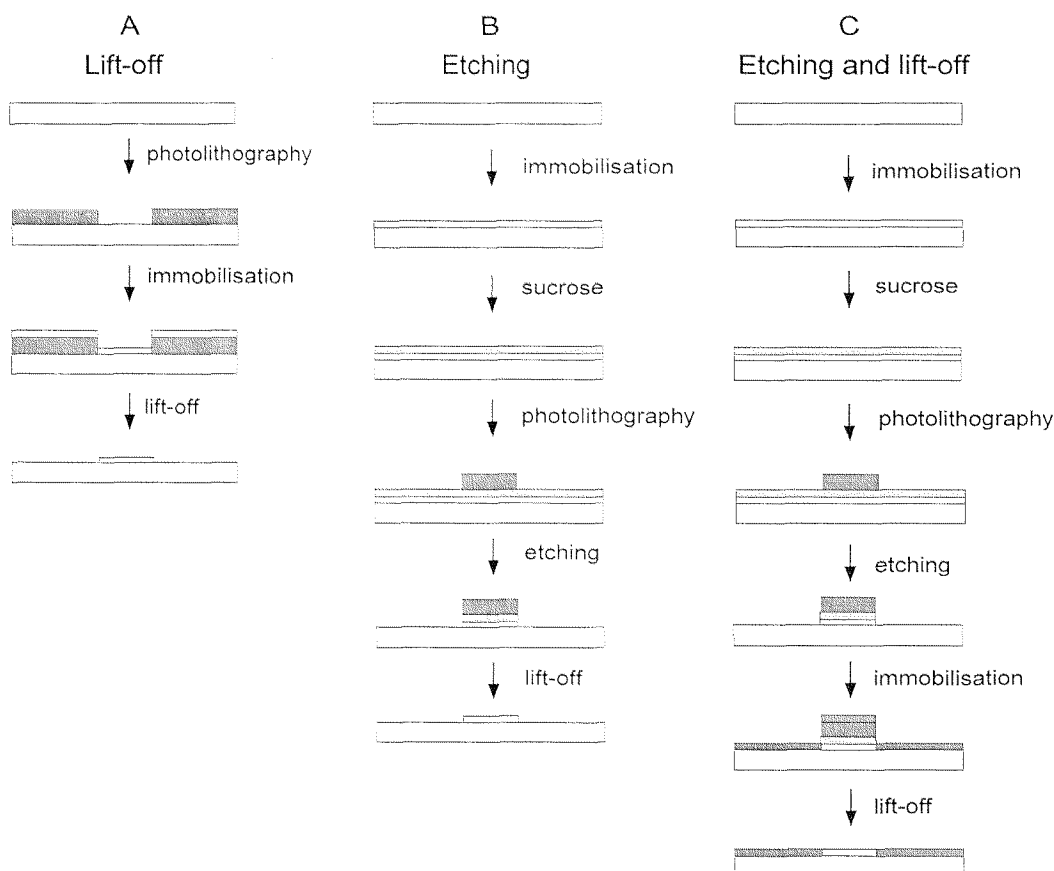
Figure 5: Photolithographic methods for the generation of protein patterns

Protein patterns were produced with two different procedures. The lift-off method (A) starts with a structured photoresist, followed by protein immobilisation and lift-off. With the etching procedure (B) a sucrose film was applied over the immobilised protein for protection. A structured photoresist was then used as a mask in the following dry etching step. A combination of these two processes is shown in C. After etching and before lift-off a second molecule can be immobilised leading to complementary protein patterns.

The described method for the etching process (Fig. 5B) was adapted from Flounders et al. (1997). Proteins were immobilised on glass chips as described in 3.2.1 and 3.2.2. The chips were then incubated in a 2% (w/w) sucrose solution in H_2O during 30 min. The sucrose solution was spin dried with a photoresist spinner (10000 rpm, 60 s) and cured in an oven

(39 °C, 1h). A positive resist (S-1813, Shipley) was applied on each chip (2500 rpm, acceleration 1000 rpm/s, 45 s) and soft-baked on a hotplate during 1 min at 90 °C. The chips were exposed through a mask (mercury lamp 350–450 nm) during 8 s and developed (MF-319, Shipley; 10 s). Development was stopped by soaking in water for a few seconds. Exposed protein was then removed in an oxygen plasma etch (100% O_2, 400 s; BMP Plasmatechnologie GmbH, Germany). If no second molecule was immobilized the photoresist was now removed by ultrasonic treatment in acetone during 2 min. Otherwise, the second protein was immobilized using isooctane as a solvent for the silanisation step (Fig. 5C). After immobilization of the second protein the photoresist was removed with acetone as described above.

2.2.6 Staining of immobilised proteins

Nonspecific binding sites on the chip were blocked by soaking the chips in tris buffered saline (TBS; 137 mM NaCl, 2.7 mM KCl, 25 mM Tris) containing 5% milk powder during 30 to 60 min while shaking. The chips were washed twice with 0.1% tween 20 (Fluka) in TBS during 5 min. Detection of immobilised rabbit-antibody (rIgG; Sigma) was done with rhodamine (TRITC) labelled goat-anti-rabbit antibodies (Sigma) diluted 1:500 in TBS supplemented with 0.1% tween 20 and 3% milk powder. Streptavidin detection was done with biotin-fluorescein (50 mg/ml in the same buffer; Sigma). Immobilised Cys-axonin-1 was immunostained using R50-rabbit-anti-axonin-1 antibody (kindly provided by P. Sonderegger, Zürich) and a fluorescein (FITC) labelled goat-anti-rabbit antibody (Cappel, Organon Teknika Corp., USA). These solutions were incubated during 2 h. Finally the chips were washed twice with 0.1% tween in TBS, mounted on a coverslip and examined with a fluorescence microscope (Zeiss, Axiophot; FITC λ_{ex} = 495 nm, λ_{em} = 525 nm; TRITC λ_{ex} = 552 nm, λ_{em} = 570 nm) equipped with a CCD camera (Kappa CF8/1 DXCK2IS, Germany).

2.3 Results

2.3.1 Characterisation of microstructured chips

The produced chips were inspected with a microscope to reject chips with fabrication defects. Most defects were found in the gold lanes, probably due to the poor adhesion of the gold film on the glass substrate. Samples to be investigated with the scanning electron microscope were sputtered with a thin layer of gold. Fig. 6 shows micrographs of the chip

at different magnifications to illustrate the chip design, the alignment of the grooves and their structure.
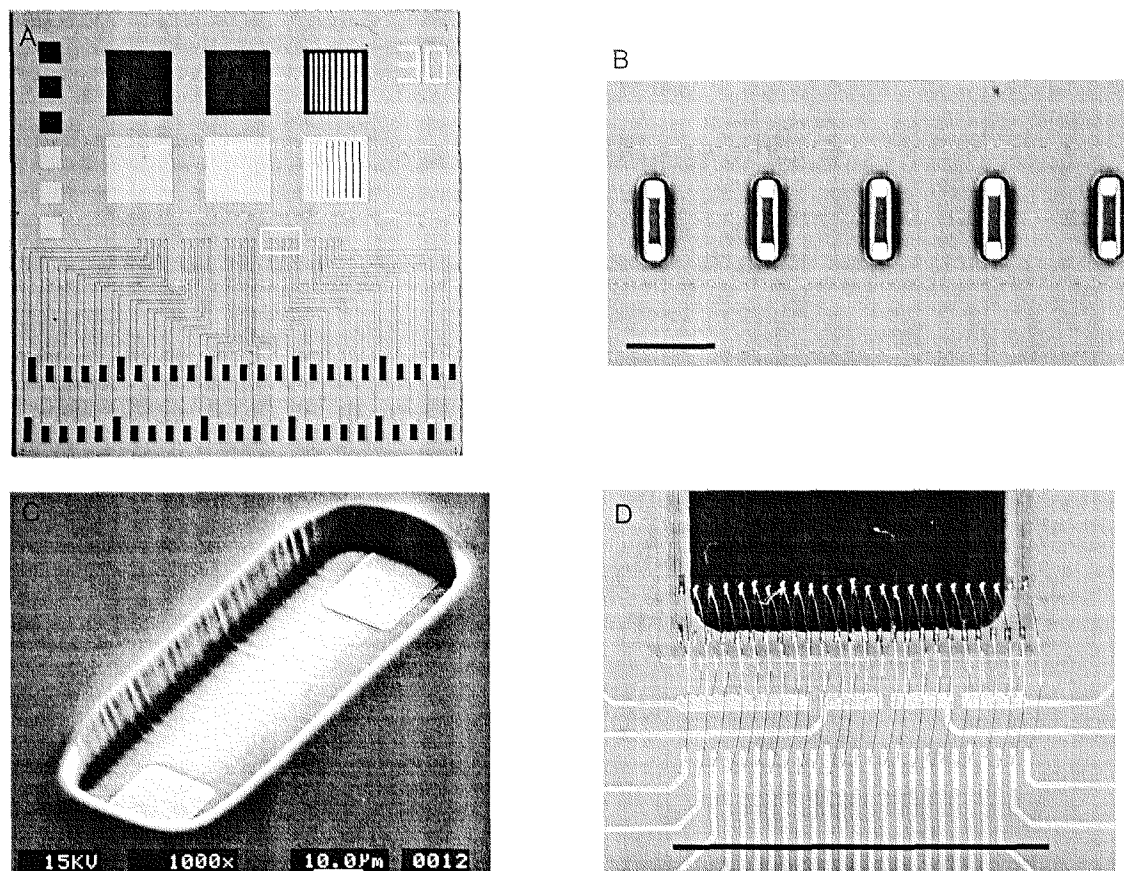
Figure 6: Microstructured chip

(A) Overview of whole chip (side length 10 mm). The grooves with electrodes are in the centre of the chip, at the bottom part are the contact pads for the bonding and the top part of the chip has areas of gold and glass for testing the immobilisation. (B) Epi-illumination light micrograph of five microgrooves (white box in A) with gold electrodes and conducting tracks visible under the polyimide film (scale bar 100 μm). (C) Scanning electron micrograph of one microgroove with gold electrodes at each end and polyimide walls (scale bar 10 μm). (D) Chip (dark area) bonded to contact pads on printed circuit board with Al-wires (scale bar 10 mm).

With electrochemical measurements it could be shown that the conduits between the soldered wire on the printed circuit board and the gold electrode on the chip were intact (Fig. 7). If more than one microelectrode was contacted the measured current increased. No crosstalk between neighbouring electrodes could be seen within the sensitivity of the equipment used.

Figure 7: Cyclic voltamogram of ferrocene-caproylamine measured with the extra-cellular gold electrodes
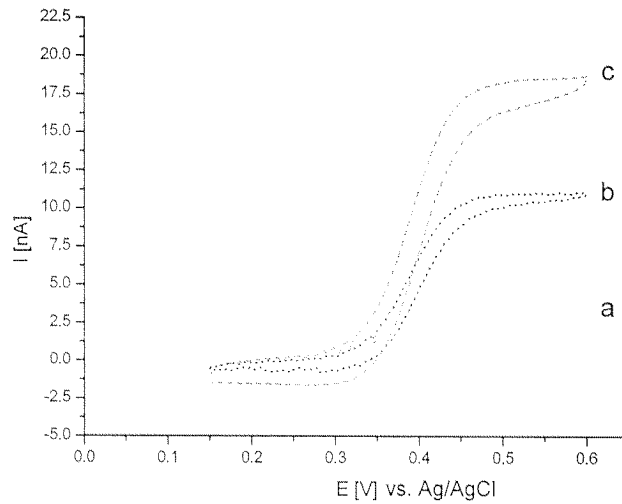
The curves represent measurements with one (a), five (b) or ten (c) gold electrodes.

Once the chips were bonded to the printed circuit board, they were reused several times for the immobilisation of adhesion molecules and culturing of cells. With the described cleaning protocol the chips could be reused up to ten times for immobilisation and cell culture (4–6 d in culture), then the isolating silicon nitride layer would start to detach from the underlying gold lanes, leading to short circuits. It was not clear if the detachment of the silicon nitride was due to poor adhesion to the gold, or to corrosion processes due to cell media and culturing, or a combination of both. The sputtered Si_3N_4 was not pin-hole free, and this holes could be a cause for leakage of ions into the layer.

2.3.2 Patterning proteins with lift-off and etching methods

In the lift-off method the photoresist was first applied to the surface and photolithographically structured (Fig. 5A). The protein was then immobilised on the sample and the resist structure was removed using a resist remover. A main constraint in this technique resulted from the used protein immobilisation technique. Organic solvents such as toluene used for silanisation attacked the photoresist structure. Therefore, for the immobilisation of the proteins isooctane was used as solvent for the silanes. The pattern resolution in this method is mainly given by the photoresist structure. Fig. 8 shows images of a photoresist test structure

(Fig. 8A) and a fluorescence image of rIgG pattern resulting after lift-off and immunostaining (Fig. 8B). Down to 2 µm line widths no significant loss of resolution was found for the transfer of the pattern into the protein layer.
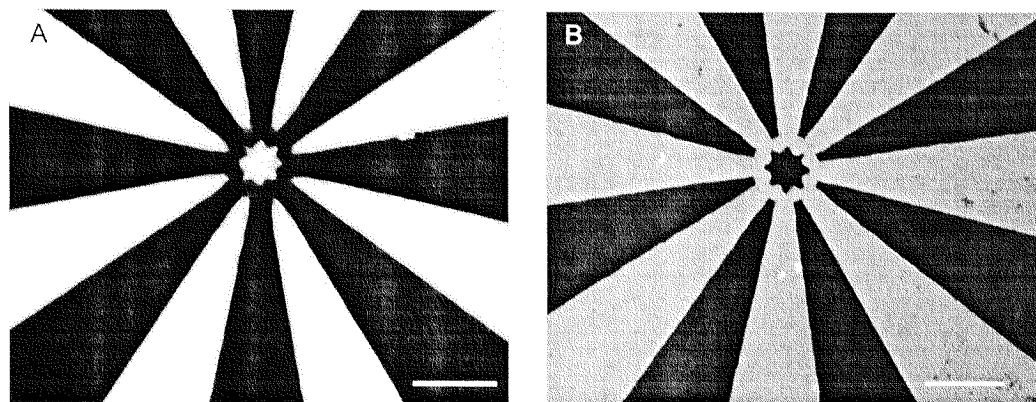

Figure 8: Pattern resolution of lift-off method

Fluorescence micrographs of photoresist structure (A) and the corresponding rIgG pattern (B) after lift-off and staining with a TRITC-labelled anti-rIgG antibody. The photoresist in (A) is auto-fluorescent at this excitation wavelength (552 nm). Scale bars 20 µm.

The lift-off method was also used to locally immobilise proteins into the microgrooves of the microstructured chips. A photoresist was spun on the microchips and structured using the dark field copy of the mask used for polyimide structuring. As a test protein rabbit-antibodies were immobilised and immunostained with an anti-rabbit antibody. Fig. 9B shows that the protein was immobilised only in the microgroove.

In the etching method the structured photoresist was used as a mask during an etching step to transfer the pattern into the underlying protein film. Spinning the sucrose solution at high rotation speed for at least 1 min was essential to achieve a good adhesion of the photoresist which was applied in the next step. Otherwise, the photoresist would peel off the surface during development. Therefore, developing times had to be kept short and the samples were only gently moved. Nevertheless, fine photoresist structures such as long narrow lines, started to float on the protein/sucrose layer during the development of the photoresist and the subsequent washing. The limit of resolution of this method was therefore in the range of 2 µm. The functionality of the patterned proteins was assessed with neurite outgrowth (see Fig. 16, chapter 3).
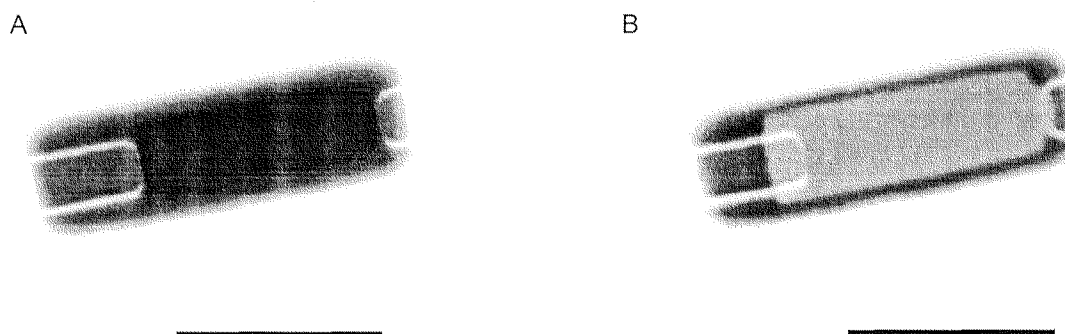
A   B

Figure 9: Localised immobilisation of protein in the microgrooves

IgG was immobilised at the bottom of the microgroove using the lift-off patterning method. (A) shows a fluorescence micrograph of a microgroove without immobilised antibody, in (B) the immobilised anti-body can be seen as rectangular film on the glass surface at the bottom of the groove. The surrounding polyimide is auto-fluorescent at this excitation wavelength (λ = 552 nm). Scale bar 50 μm.

2.3.3 Formation of complementary protein patterns

Two complementary protein patterns were generated starting from the same photolithographic mask when following the etching and the lift-off method, respectively (Fig. 5C). The first protein layer was patterned according to the etching method, but the photoresist was not removed. Obviously, some new limitations of the process had to be considered, as the photoresist which is protecting the structure of the first protein needed to withstand the immobilisation process of the second protein. It was found, that the amino-silane APTES used for the immobilisation of thiol-terminated molecules would attack the photoresist after the etching step. Therefore, the experimental setup had to be adapted to avoid immobilisation of the thiol-terminated protein as the second molecule. The subsequent aqueous incubation steps (crosslinker and protein) were not critical for the stability of the photoresist pattern. Fig. 10 shows the green and red fluorescence images of complementary line patterns of streptavidin and rabbit-IgG. In this experiment streptavidin was immobilised as the first protein and structured by etching while the IgG was immobilised as the second protein and structured by lift-off. For visualisation the sample was incubated with a mixture of biotin-fluorescein and a TRITC-labelled anti-rIgG antibody which bind selectively to the avidin and the rabbit-IgG, respectively. A clear pattern definition was found for 5 μm lines of both proteins, but the 2 μm patterns seem to be the limit of resolution of the combined process.
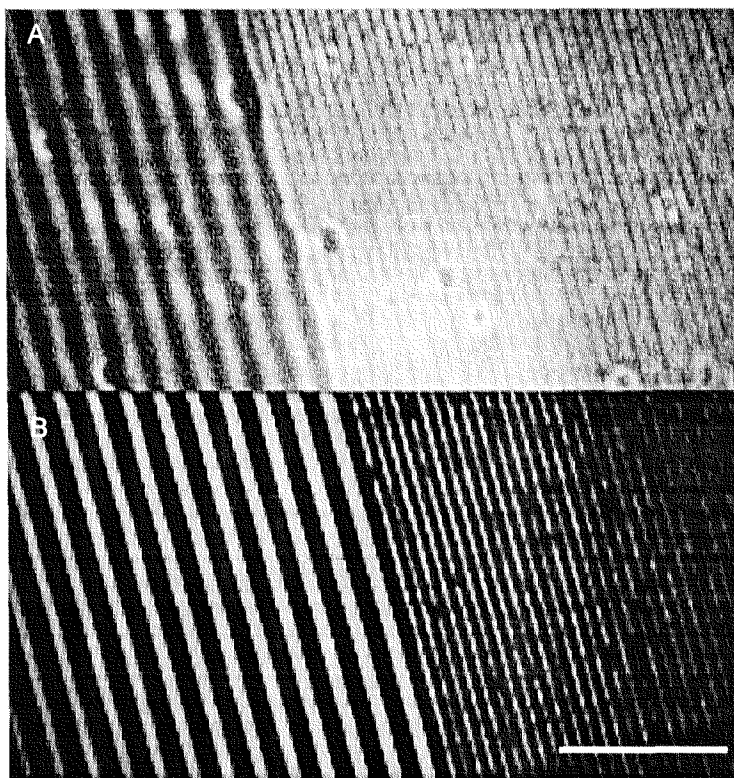
Figure 10: Complementary patterns of streptavidin and rIgG

Fluorescence micrographs of streptavidin and rIgG patterns taken at the same position. Streptavidin (A) was patterned with the etching method and rIgG (B) using the lift-off method. Biotin-fluorescein (A, green) and anti-rabbit IgG-TRITC (B, red) were used to visualize the line patterns (left 5 μm, right 2 μm line width). Scale bar 50 μm.

2.4 Discussion

2.4.1 Microstructured chip

The layout of the described microstructured chip was designed for testing and evaluation purposes. Half of the chip surface with different areas of gold and glass was dedicated to develop the immobilisation procedure which however was then done on unstructured chips.

The biocompatibility of the materials in contact with cell media and cells is a prerequisite for the establishment of cell cultures. The materials on the chip (glass, gold and polyimide) were all compatible with cell culturing. But also further material present on the chip used for bonding and embedding should not inhibit cell growth. This was not the case with the embedding resin (H70E/H70E-2; Polyscience AG, Cham, Switzerland) employed for protection of the bond wires in the first batch of chips. Therefore, further chips were embedded in PDMS which was known to be cell compatible from earlier experiments. The material has to be not only biocompatible but it must also to be inert versus the agents used for the immobilisation procedure and also in cell culturing. For example it was observed that during the silanisation procedure with APTES in toluene the PDMS would swell and the APTES would attack it, forming a persistent film of PDMS/silane on the glass. All attempts to remove this opaque film on the chip surface failed. Therefore, the silanisation was done in ethanol and in order to protect the PDMS from the silane a small glass ring was glued on the chip (see Fig. 23).

The cell culture medium is a buffer with many different ionic substances. This solution was very corrosive with the copper contacts on the print board and also with the bond wires if they were not perfectly embedded in PDMS. Recently, an extensive study on passivation and corrosion of microelectrode arrays has been published (Schmitt et al., 1999). Best long-term results were obtained if the conducting lanes and electrodes were buried into the silicon and they were passivated with triplex layers of $SiO_2/Si_3N_4/SiO_2$ (130/540/130 nm). The failure of the Si_3N_4 passivation layer seen in the bonded chips was probably due to pinholes in the film, poor adhesion on gold or mechanical stress.

2.4.2   Protein patterning

A new method to generate protein patterns using photolithographic techniques has been developed. In the lift-off method in which the photoresist structure is removed together with the overlying parts of the protein layer, the impact of the remover solution on the protein must be considered. Organic solvents such as acetone may be used as well as water based resist removers which usually contain amines or alkali-hydroxides at a pH of 9 to 11. This restricts the applicability of the lift-off process to small peptides and relatively robust proteins such as avidin or various antibodies. Many groups have thus used this patterning technique only to pattern silanes with different functionalities onto which directed immobilisation of proteins was possible after lift-off. This work presents an adaptation of photolithographic techniques for the patterning of multidomain cell adhesion proteins. Embedding the protein film in a sucrose layer protects the proteins from denaturation. The sucrose maintains a suitable environment for the proteins throughout the process and it efficiently protects the protein from direct contact with organic solvents. It becomes possible to create patterns of sensitive proteins such as axonin-1 and NgCAM. Due to the lower adhesivity of the photoresist layer on the sucrose-embedded protein the pattern resolution

is reduced. Photolithographic processes are compatible with thin-film technology. Therefore it is possible to align the protein structures with high precision allowing large scale production. Patterning of two proteins on one surface has been presented here. In principle it should be possible to add patterns of further proteins on the same substrate by subsequent treatments with sucrose, photoresist application etc. However, the more steps that are added, the more problems with protein stability and pattern resolution may arise. Also, it was found that the photoresist would be dissolved by the APTES in the combined etching/lift-off process. This was only the case if protein was previously immobilised. The experimental proceeding has therefore to be carefully planned.

The presented technique has some disadvantages that cannot be neglected when comparing with different patterning techniques for the use in common neurobiological or biochemical laboratories. Expensive equipment is needed compared to cheaper patterning procedures such as microstamping or UV-ablation. Alignment to preformed structures is however easier to handle: a mask-aligner is perfectly suitable for precise alignment.

Table 2 lists the most popular protein patterning techniques with their limits of resolution and major advantages and disadvantages.

Table 2: Overview of protein patterning techniques

Patterning technique	Patterned molecules	Resolution	Advantages	Disadvantages	Applications
Photolithography	silanes[a], antibodies[b], axonin-1[c]	2 μm	compatible with thin film technology; parallel production; exact pattern definition; multiple protein patterning	expensive equipment; high number of process steps	large scale production, biochips
Patterning with light	silanes[d], self-assembled monolayers[e], laminin[f]	< 1 μm	one process step; cheap equipment;	only two complementary patterns;	lab-scale
Microcontact printing	silanes[g], thioalkanes[h], polylysine[i]	200 nm	cheap equipment; reusable stamps; can be combined with covalent immobilisation; multiple protein patterns	small scale production; alignment with existing microstructures; reproduction	lab-scale
Microfluidic networks	antibodies[j], polylysine[k], cells[l]	3 μm	multiple number of proteins can be patterned in one step in different patterns	small scale production; alignment with existing microstructures	lab-scale

a. Kleinfeld et al., 1988
b. Flounders et al., 1997
c. this work
d. Matsuzawa et al., 1996
e. Vaidya et al., 1998
f. Hammarback et al., 1985
g. Kane et al., 1999; Pompe et al., 1999
h. Mrksich and Whitesides, 1995
i. Branch et al., 1998
j. Delamarche et al., 1997
k. Martinoia et al., 1999
l. Chiu et al., 2000

Seite Leer /
Blank leaf

3

Functionalised Glass Surfaces for Neuron Cultures

3.1 Introduction

3.1.1 Neural cell adhesion molecules

Extending neurons in the developing nerve system find their targets by sending out their axon and dendrites along guidance cues presented locally in the extracellular fluid, on cells or in the extracellular matrix (ECM). This guidance cues can be soluble molecules (long range guidance cues) or membrane bound molecules (short range guidance cues) which are recognised by receptor proteins on the axonal surface (Fig. 11).

Long-range guidance cues are secreted by target tissues. They can form gradients which act on growing nerve tips. The same molecule can function as an attractive or a repulsive cue, depending on the neuronal population or the developmental state (Tessier-Lavigne and Goodman, 1996). Membrane and ECM bound proteins act as short-range guidance cues. Two large families of neural cell adhesion molecules (CAMs) are involved in axon guidance: The cell adhesion molecules of the immunoglobulin (Ig) superfamily (Rathjen and Jessel, 1991; Grumet, 1991; Sonderegger, 1998) and the cadherins (Takeichi, 1991). The neural CAMs of the Ig-superfamily are membrane glycoproteins which act as local guidance cues mediating target recognition and/or linear neurite extension. Many of these molecules undergo homophilic interactions. Some members are also involved in heterophilic interactions with other CAMs or molecules of the extracellular matrix (for a review see Sonderegger, 1998). The members of the cadherin family undergo homophilic interactions in a calcium-dependent manner (Takeichi, 1991).

A second important group of adhesion molecules is associated with the ECM and is responsible for cell-substrate adhesion. These large extracellular glycoproteins consist of two iden-
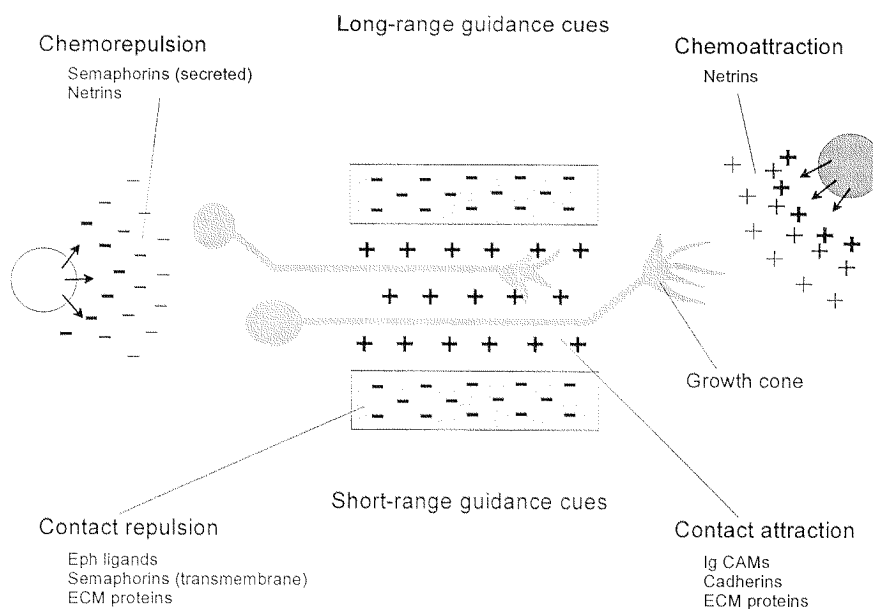
Figure 11: Guidance of neurons in vivo

Four types of mechanisms contribute to guiding growth cones: contact attraction, chemoattraction, contact repulsion and chemorepulsion. Contact attraction and contact repulsion are mediated by short-range or local guidance cues, i. e. membrane bound proteins. In contrast, chemoattraction and chemorepulsion are mediated by long-range cues which are secreted diffusible molecules. Examples of ligands implicated in mediating each of these mechanisms are provided. Note that the same molecule can act as repulsive and attractive cue, depending on the neuronal population and the developmental state. Adapted from Tessier-Lavigne and Goodman, 1996.

tical or similar polypeptide chains hold together via a disulfide bridge. They interact with cell bound integrins, a family of receptors that recognises various ligands depending on the combination of different subunits present (Reichhardt and Tomaselli, 1991). Members of the ECM associated adhesion molecules are: laminin, fibronectin, tenascin and thrombospondin.

The chemistry of the substrate, however, is not the only guiding influence to which a growth cone responds. The topography of the surface is also important: growth cones sticking to fibres, for example, will tend to follow their orientation - a phenomenon known as contact guidance.

Furthermore, during the last years there has been growing evidence that cell adhesion molecules also play important and diverse roles in regulating synaptic plasticity, learning and memory (Benson et al., 2000).

3.1.2   The neural cell adhesion molecules of the Ig superfamily

The axonal membrane proteins of the Ig-superfamily (reviewed in Sonderegger, 1998) can be further classified by the number of Ig- and fibronectin type III (FNIII)-related domains (IgFNIII-like proteins; Sonderegger and Rathjen, 1992). F11/F3 and axonin-1/TAG-1 with six Ig-like and four FNIII-like repeats belong to one subclass, whereas L1/NgCAM, NrCAM and neurofascin with six Ig- and five FNIII-like domains represent another sub-group. NCAM with five Ig- and two FNIII-like repeats cannot be assigned to these sub-groups.

3.1.3   Axonin-1

Members of the axonin-1/TAG-1 family have been found in chicken, mouse, rat and humans. These adhesion proteins are expressed in differential patterns in neurons during neural development (Yoshihara et al., 1995). Axonin-1 is involved in neurite outgrowth (Stoeckli et al., 1991), axonal pathfinding (Stoeckli and Landmesser, 1995; Stoeckli et al., 1997) and neurite fasciculation (Ruegg et al., 1989; Stoeckli et al., 1991; Kunz et al., 1996; Kunz et al., 1998). The proteins of the axonin-1/TAG-1 family exist as GPI-anchored and as soluble form. Studies on the release mechanism of axonin-1 suggest that part of the sol-uble axonin-1 is released from the membrane by a phosphatidylinositol-specific phospho-lipase D (Lierheimer et al., 1997). Axonin-1 can undergo homophilic binding (Rader et al., 1993) and a number of heterophilic interactions with NgCAM (Kuhn et al., 1991), NrCAM (Suter et al., 1995; Fitzli et al., 2000), β-integrin (Felsenfeld et al., 1994), neurocan, phospha-can/protein tyrosine phosphatase-ζ/β, NCAM (Milev et al., 1996). The interaction of axonin-1 with NgCAM occurs in the plane of the same membrane (cis) as domain deletion and crosslinking experiments revealed (Kunz et al., 1998; Fig. 12A). This heterodimer is thought to interact with an axonin-1/NgCAM cis-heterodimer on another cell forming an axonin-1$_2$/NgCAM$_2$-tetramer which is probably involved in activation of intracellular sig-nalling pathways as their association with kinases suggests (Kunz et al., 1996).

The binding of axonin-1 on neural cells to NrCAM on glial cells assures a close neurite/glia contact. Suter et al. (1995) suggest a role of this complex during the initial state of axon ensheathment in the peripheral neural system. The relevance of the interaction of axonin-1/ TAG-1 with NCAM, neurocan, phosphacan and β1 integrin is still unclear.

Structural studies on axonin-1 have revealed that a glycine/proline rich segment between Ig-domains and the membrane proximal FNIII-like repeats may form a flexible hinge region that folds the protein back to a horseshoe-like structure in the unbound state (Rader et al., 1996). The crystal structure of the ligand binding fragment Ig1-4 has been solved recently (Freigang et al., 2000). The overall structure of the axonin-1(Ig1-4) is U-shaped due to contacts between domains 1 and 4 and domains 2 and 3. The domain arrangement found

in the crystal suggests that the cell adhesion by homophilic axonin-1 interaction occurs by the formation of a linear zipper-like array in which the axonin-1 molecules are alternately provided by the two apposed membranes (Fig. 12B).
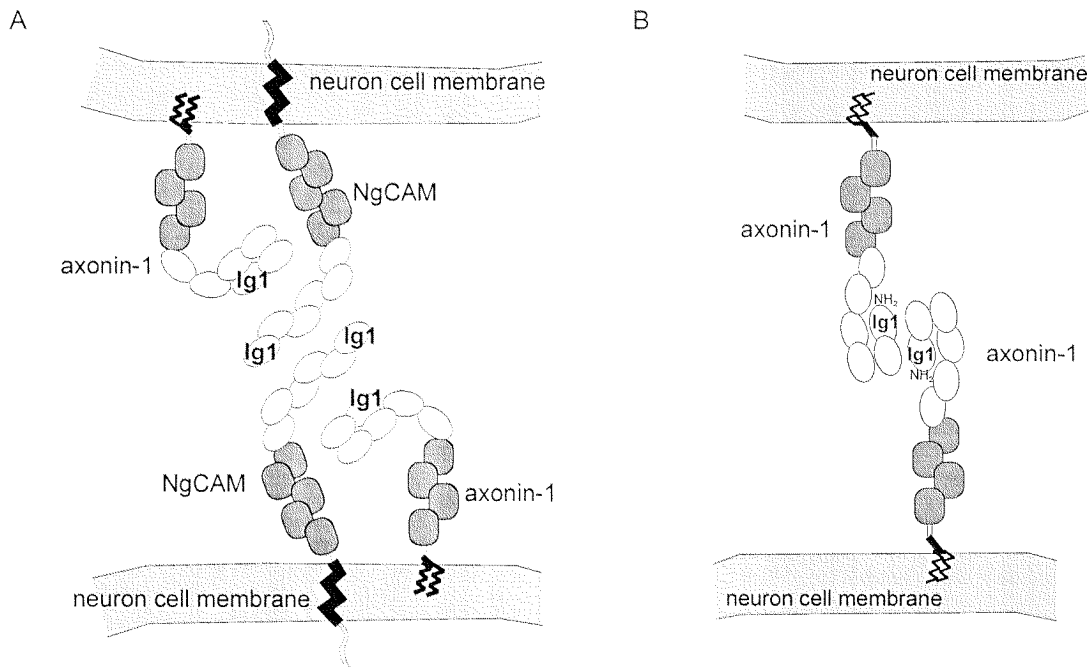

Figure 12: Binding models of heterophilic and homophilic axonin-1 interaction

(A) Axonin-1 and NgCAM interact in the plane of the same membrane. An axonin-1_2/NgCAM$_2$-tetramer is formed between two apposed cell membranes. Adapted from Kunz et al., 1998. (B) Model of the homophilic axonin-1 binding as suggested by the crystal structure of axonin-1(Ig1-4). A zipper-like organisation in the membrane of two apposed cells is suggested. Adapted from Freigang et al., 2000.

3.1.4   NgCAM

Chicken NgCAM is regarded as closely related to mammalian L1 (Sonderegger and Rathjen, 1992; Sonderegger, 1998). Members of the NgCAM/L1 family of Ig/FNIII-like proteins have been described for invertebrates and vertebrates. In many species different splice isoforms of the same gene product are generated by alternative splicing (Davis et al., 1993; Grumet et al., 1991; Takeda et al., 1996). However, it is not known whether these isoforms have specialised functions. The molecules of the NgCAM/L1 family are predominantly expressed in the developing and adult central and peripheral nervous system. Splice forms missing the RSLE-peptide sequence in the middle of the cytoplasmic domain are found to

mediate cell interactions outside the nervous system where they mediate interactions with integrins (Ruppert et al., 1995; Montgomery et al., 1996; Takeda et al., 1996). During development different neuronal and glial cell populations express the different members of this family in a complex spatio-temporal pattern (Moscoso and Sanes, 1995). Studies indicate that these proteins are involved in axonal pathfinding, axonal outgrowth, neurite fasciculation, neuronal cell migration, myelination and synaptic plasticity. These functions are mediated by interactions of the members of the NgCAM/L1 family with a wide variety of other proteins. Apart from homophilic binding (Grumet and Edelman, 1988), the extracellular part of NgCAM interacts with axonin-1 (Kuhn et al., 1991), F11/contactin (Brummendorf et al., 1993), laminin (Grumet et al., 1993), neurocan (Friedlander et al., 1994), phosphacan/ protein tyrosine phosphatase-ζ/β (Milev et al., 1994), and NrCAM (Lustig et al., 1999). The short cytoplasmic domain interacts with ankyrin (Davis and Bennett, 1994), casein kinase II, and S6 kinase p90Rsk (Kunz et al., 1996) indicating an implication in signal transduction.

3.2 Methods

Buffer media and solvents were purchased from Fluka or Merck and were all high purity grade.

3.2.1 Immobilisation of thiol-terminated molecules

The recombinant adhesion proteins Cys-axonin-1 and Cys-NgCAM were produced by Dr. Lukas Leder, Institute of Biochemistry, University of Zürich (now Novartis, Basel; Sorribas et al., 2001). In order to achieve covalent and oriented immobilization of the neural cell adhesion proteins axonin-1 and NgCAM on glass or gold surfaces, the transmembrane and intracellular domains of the proteins were deleted and a cysteine was inserted by genetic engineering at the C-term of the last extracellular domain near the membrane. This modification allowes the secretion of the recombinant proteins and also a covalent immobilization via the thiol group of the cysteine on glass using silane chemistry and a maleinimide cross linker or on gold directly (Fig. 13A).

Glass chips (1×1 cm; Hoya) were cleaned with acetone and isopropanol before use. The surface was activated with concentrated HNO_3 during 3 minutes and then rinsed with H_2O. The chips were silanised during 1 h in a 2% aminopropyltriethoxysilane (APTES; Sigma) solution in toluene, washed with toluene and dried with a stream of nitrogen. Chips with photoresist structures were silanised with isooctane; chips embedded in PDMS were silanised with ethanol as solvent. For the immobilization of the cysteine terminated recombinant proteins (Cys-axonin-1 and Cys-NgCAM), and the adhesion peptide Arg-Gly-Asp-Cys (RGDC) the following protocol was used: a 5 mM solution of the heterobifunctional

crosslinker N-[γ-maleimidobutyryloxy]sulfosuccinimide ester (sGMBS; Pierce) was prepared by dissolution in 30 μl dimethyl sulfoxide and dilution in 50 mM phosphate buffer pH 7.0. 75 μl thereof were applied on each chip. The samples were rinsed with phosphate buffer after 2 h incubation and dried with nitrogen. The recombinant adhesion proteins Cys-axonin-1 and Cys-NgCAM were diluted to a final concentration of 250 μg/ml in 50 mM phosphate buffer pH 7.4. A 2 mM solution of RGDC (Bachem, Switzerland) was prepared in 50 mM phosphate buffer pH 7.0. The protein or peptide solutions (75 μl) were applied on the chips for 2 h and the chips were then rinsed with phosphate buffer. If the applied solutions had not been sterilised previously (0.2 μm filter, Millipore) the chips were sterilised with 70% ethanol/H_2O (filtered sterile with 0.2 μm filter) before use as cell culture substrate.

Gold-chips produced as described in 2.2.1 were cleaned with acetone and isopropanol and introduced into the chamber of a plasma etcher (BMP Plasmatechnologie GmbH, Germany). The gold surface was exposed to an oxygen plasma for 3 min to clean it from deposited material. Afterwards, the freshly etched surface was treated with a 5 mM solution of mercaptoethanesulfonate (MES; Fluka) in ethanol/H_2O (50% v/v) to prevent fouling. After 1 h incubation the chips were washed and then dried with N_2. Protein solutions were prepared as described above and applied on the chips and after 2 h the chips were washed with buffer.

3.2.2   Immobilisation of molecules with free amino-groups

For proteins with no terminal cysteine the amino groups of the lysine residues were linked to a hetero-bifunctional crosslinker. A protein-crosslinker conjugate was prepared as follows: 400 μg protein (streptavidin or rIgG, both from Sigma; 200 μg/ml final concentration) and 0.25 mM *m*-maleimidobenzoyl-N-hydroxysulfosuccinimide ester (MBS; Pierce) in 50 mM phosphate buffer pH 7.4 were reacted for 2 h and then dialysed against 50 mM phosphate buffer pH 7.0. This conjugate solution was applied on glass chips previously silanised with 2% mercaptopropyltriethoxysilane (MPTMS; Fluka) in toluene (or in isooctane if a photoresist film was on the chip) for 2 h and then washed with phosphate buffer.

3.2.3   Patterning of RGDC and Cys-axonin-1

Patterns of RGDC were produced with the lift-off method (2.3.2), whereas Cys-axonin-1 patterns were produced using the etching method (2.3.2). Patterns of parallel lines and grids with different line widths (5, 10, 15, 25 μm) and at different distances were generated. Immobilisation procedures were as described above. The lift-off step in acetone served also to sterilise the chip.
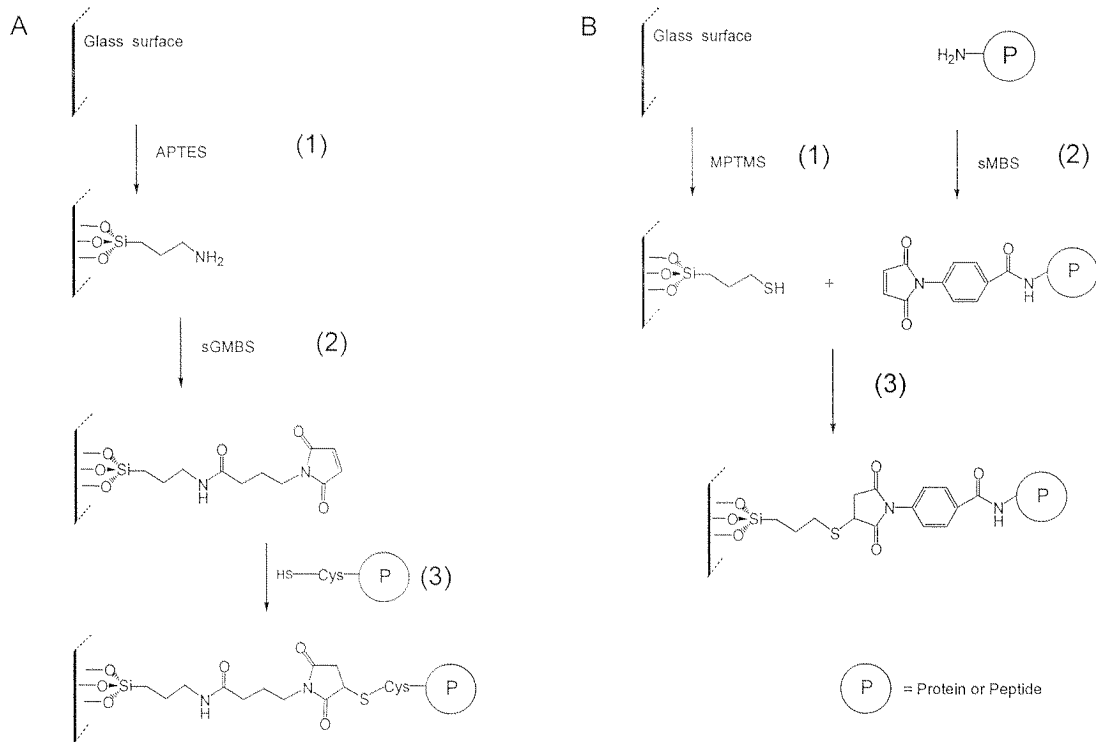
Figure 13: Covalent immobilisation of molecules on glass using silane chemistry

(A) Immobilisation scheme for thiol-terminated molecules. Aminosilane is bound to a cleaned glass surface (1), then the heterobifunctional crosslinker sGMBS binds to the free amino-group on the surface (2). The maleimide-group on the immobilised crosslinker will then react with free thiol groups (3), leading to a covalent and oriented immobilisation of the adhesion molecule.

(B) Immobilisation of proteins with free amino-groups. The glass surface is silanised with a mercapto-silane (1). The previously synthesised crosslinker-protein conjugate (2) is then bound to the surface (3), leading to a covalent, but not oriented immobilisation of the protein.

3.2.4   Coating with laminin and polylysine

75 µl of a 40 µg/ml mouse laminin (GibcoBRL) solution in phosphate buffered saline (PBS) or of a 100 µg/ml poly-L-lysine (Sigma) solution were applied on the chips or on tissue culture dishes (Nunc) and incubated at 37 °C. After 2 h the chips were rinsed with PBS.

3.2.5   Reduction of nonspecific binding of proteins and cells

Glass surfaces were treated with various silanes to reduce protein adsorption and cell attachment. Cleaned glass chips were incubated for 1 h in 2% solutions of octadecyltrichlorosilane (ODS; Aldrich, USA) or tridecafluoro-1,1,2,2-tetrahydrooctyl trichlorosilane (TFS; ABCR, Germany) in dry hexane and subsequently washed with the solvent. 1 mg/ml O-[2-(Trimethyloxysilyl)ethyl]-O'-methyl-polyethylene glycol 5000 (PEG-silane; Fluka) solution in H_2O was incubated on the chips for 1 h and the chips were then washed with H_2O.

3.2.6   Determination of surface density of proteins

Radiotracer techniques were used to determine the surface coverage of immobilised adhesion molecules. Radiolabelled ^{125}I-tracer molecules were synthesised as follows. 200 µl iodogen-solution (1.6 mg Iodo-Gen; Pierce, in 4 ml ethyl acetate) was dried with nitrogen in a glass test tube. Then, 250 µl of a 200 µg/ml protein solution in phosphate buffer pH 7.4 and 200 µCi of ^{125}I (NEN, Belgium) were added, vortexed and reacted in ice water for 15 min. The reaction was stopped by transferring the solution to a new test tube containing 200 µl elution buffer (0.5 µg/ml protein in phosphate buffer pH 7.4). Labelled proteins were purified with a gel filtration column (PD10, Pharmacia). Per chip about 100000 cpm of the radiolabelled protein were added to the unlabelled protein solution. The activity bound to the chips was determined with a gamma-counter (LB2111, EG&G Berthold, Germany) and activity distribution on the surface was visualised exposing the chips in an electronic autoradiography instrument (InstantImager, Canberra Packard) or on imaging plates (Fuji BAS2500, Japan).

3.2.7   Buffers and media for cell culturing

PBS-:

    8 g   NaCl (Fluka 71380); f. c.[a] 136.9 mM
  0.2 g   KCl (Fluka 60130); f. c. 2.7 mM
  1.44 g $Na_2HPO_4 \times H_2O$ (Merck 6580); f. c. 8.1 mM
  0.2 g KH_2PO_4 (Merck 4873); f. c. 1.5 mM
          to 1 l with H_2O; filtered sterile (0.2 µm; Mediakap-5, Microgon)

a.   f. c.: final concentration

PBS:

    0.13 g $CaCl_2 \times 2H_2O$ (Fluka 21098); f. c. 0.9 mM

    0.10 g $MgCl_2 \times 6H_2O$ (Merck 5833); f. c. 0.5 mM

        in 1000 ml PBS-; filtered sterile (0.2 µm filter, Microgon)

Maintenance solution (Erhaltungslösung):

0.5% D-glucose (Fluka 49140) in PBS

Trypsinisation solution:

    0.5 ml Trypsin (1 mg/ml; GibcoBRL 25095-019)

    4.5 ml 0.5% D-glucose (Fluka 49140) in PBS-

Medium supplements

Albumax:

Albumax I (low IgG, low endotoxin, GibcoBRL 066-01020 E), 250 mg/ml in PBS-

N3-Supplement:

    8 ml 10 mg/ml BSA (68 kD, Sigma A-9418) in PBS-; f. c. 15 µM

    0.8 ml 2 mg/ml corticosterone (Sigma C-2505) in ethanol; f. c. 60 µM

    3.2 ml 25 mg/ml insulin (Sigma I-5500) in 25 mM HCl; f. c. 174 µM

    0.8 ml 400 µM progesterone (Sigma P-0130) in ethanol; f. c. 4 µM

    3.2 ml 500 mM putrescine (Sigma P-7505) in PBS-; f. c. 20 µM

    8 ml 10 µg/ml Na-selenit (Sigma S-1383) in PBS-; f. c. 6 µM

    8 ml 0.1g/ml holo-transferrin bovine (Gibco 11107-026) in PBS-; f. c. 100 µM

    8 ml 200 µg/ml trijodothyronin (Calbiochem 64245) in ethanol; f. c. 3 µM

        volume adjusted to 80 ml with PBS-; filtered sterile (0.2 µm filter, Millipore)

        and 250 µl aliquots stored at -20 °C

NGF:

30 µl rhu-β-NGF (Genentech 11778/32, USA; 0.83 mg/ml) to 1 ml with 1 mg/ml BSA in PBS-

Glutamine:

L-Glutamine (Sigma G-3126); 200 mM in H_2O, filtered sterile (0.2 µm)

Minimal essential medium stock solution(MEM):

1 P	MEM w/o glutamine (GibcoBRL, 072-90011N)
4 l	ultra high pure H_2O
11 g	$NaHCO_3$ (Fluka p.a. 71628)
0.95 l	ultra high pure H_2O

pH adjusted to 7.2 with 6 N HCl

osmolarity adjusted to 325 ± 5 mOsm by adding glucose (D-glucose; Fluka 49140); filtered sterile (0.2 µm; Mediakap-5, Microgon)

Preparation of MEM for cell cultures:

25 ml	MEM stock solution
500 µl	Albumax
250 µl	N3-supplement
250 µl	Glutamine
20 µl	NGF

filtered sterile (0.2 µm; Millipore), and put in incubator (37 °C, 10% CO_2, humidified; Brouwer SWJ300 DVBB, USA) for equilibration of pH and temperature

3.2.8   Cultures of dissociated chicken DRG neurons

Serum free minimal essential cell medium (MEM; Stoeckli et al., 1996) was prepared as described above and put into a humidified cell incubator (37 °C, 10% CO_2) for temperature and pH stabilisation. Dorsal root ganglia (DRG) were dissected from 10-day old chicken embryos as described by Sonderegger et al. (1985). The isolated ganglia were maintained in solution on ice (Erhaltungslösung, see above). The ganglia were transferred to a sterile tube with a pasteur-pipette and were dissociated during a 15 min incubation in 0.25% trypsin in PBS- (see above) at 37 °C, followed by mechanical dissociation with a pipette tip. Dissociated cells were suspended in the pre-incubated cell medium and plated on the chips at a density of 5000 cells/cm^2 for outgrowth experiments, and at 50-100000 cells/cm^2 for electrophysiological experiments. Proliferation of non-neuronal cells was minimized by the inclusion of 0.12 mM 5-fluorodeoxyuridine and 0.3 mM uridine (FUdR; both from Sigma) in the medium in some experiments. Cells were fixed with 2% formaldehyde and 0.05% glutaraldehyde (both Fluka) in MEM after 24 h incubation on the chips in a humidified incubator (37 °C, 10% CO_2).

For a characterisation of the substrate's influence on the cells, neurite outgrowth was analysed with phase contrast microscopy (Nikon Diaphot, 20× phase objective) equipped with a camera (VTE digital video high resolution camera TV11-35H). The percentage of cells with neurites after 1 d in culture was counted and the neurite lengths determined using the National Institutes of Health image software (NIH-image 1.55; http://rsb.info.nih.gov/

nih-image/download.html). Only neurites which emerged from an isolated neuron (not from a clump of cells), and which did not contact other neurites or cells, were considered. The neurite length of the longest branch was measured from the cell soma to the most remote tip.

3.2.9   Cell positioning

Three methods for the positioning of cells into the microgrooves were evaluated. The easiest way to bring cells into the grooves is to plate the cells at high density. The probability that a cell attaches to the bottom of a groove will increase with number of cells in the cell suspension. Therefore, cells were plated at 200000 cells/cm^2. The area for cell attachment was delimited by a PDMS film which had an opening of 0.5 mm × 5 mm over the grooves. As a second positioning method laser tweezers (Cell Robotics, USA on a Nikon Diaphot 300) were evaluated. Finally, a micromanipulator (TransferMan 5177, Eppendorf) equipped with a handdriven oil-pump (CellTram Oil, Eppendorf) was used for cell positioning. Glass pipettes (CG100F-10, Clark Instruments, UK) with an inner opening diameter of 30–50 μm were pulled with a micropipette puller (P-87 Puller, Sutter Instruments, USA) and polished with a microforge (MF99, Narishige, Japan). The micromanipulator was mounted on an inverted microscope stage. Positioning experiments started immediately after plating the cells on the chips. One or more cells were sucked up using the micropump, the pipette was positioned in front of a groove and the cell then gently released. When all the grooves were filled the dish was put in the incubator, however, not later than 20 min after plating.

3.3   Results

3.3.1   Surface density of immobilised adhesion molecules

The radiolabelled ^{125}I-RGDC was not stable and showed a different reactivity than the unlabelled RGDC. Therefore estimation of the surface density of immobilised RGDC was done with ^{35}S-labelled cysteine. With an applied concentration of 5 mM a surface coverage of about 100 pmol/cm^2 was found. This corresponds to 6×10^{13} molecules/cm^2. This number is in agreement with the calculations made by Huber et al. (1998) and findings by other groups (Massia and Hubbell, 1990; Dee et al., 1996) for the immobilisation of small peptide molecules.

The surface density of covalently immobilised Cys-axonin-1 as determined by radiolabelling was 400 ng/cm^2 on glass and 600 ng/cm^2 on gold when a 50 μg/ml solution of the protein was applied. These densities were the minimal densities necessary for neurite outgrowth

promotion and correspond to a dense monolayer. Repeated washing and radioactivity measurements showed that the amount of bound protein is stable during at least one month (measured period).

With half gold/half glass chips the selective binding of molecules was investigated. The thiol group of the terminal cysteine on each of the adhesion molecules allowed a direct interaction of the molecules with the gold surface. However to prevent non specific binding the gold surface was pretreated with the short chain thioalkane MES. The Cys-axonin-1 showed a 4-fold preferential binding to gold vs. glass when the chips were only treated with oxygen plasma etching and MES. If this treatment was combined with a silanisation with APTES and crosslinker binding on the gold surface was 2-fold higher than on the glass surface. It seems therefore possible to guide the thiol-terminated proteins to the gold surface although not completely preventing a coating of the glass surface.

3.3.2   Neurite outgrowth on surfaces functionalised with different substrates

DRG neurons can be identified by a typical halo around the cell body whereas glia cells appear flat. Cell debris and dead cells were observed frequently as a consequence of the preparation, but could clearly be distinguished from living cells by the phase opaque cell body.

The outgrowth of neurites on the different substrates was examined as described in the methods section and the findings are summarized in Table 3. Data in Table 3 are from three culture preparations using three chips of each substrate and are means of $n > 30$ measured neurites. Neurite outgrowth was found in 90% of the neurons when they were cultured on laminin, but only in 20% of the cells grown on the amino-terminated silane APTES. Neurite outgrowth on Cys-NgCAM was comparable to outgrowth on laminin whereas on RGDC and on Cys-axonin-1 about half of the neurons had neurites. The mean neurite lengths for each substrate were calculated for comparison. They ranged from 40 µm up to 230 µm. On APTES neurites were thick and only rarely longer than two cell diameters (Fig. 14A). On laminin and Cys-NgCAM the neurites were the thinnest and longest (Fig. 14D, E), whereas on Cys-axonin-1 (Fig. 14C), RGDC (Fig. 14B) and polylysine the neurites where slightly shorter and broader. These findings indicate that neurite outgrowth is strongly influenced by the nature of the molecules present on the surface. An influence of the underlying surface material (glass or gold) was only seen on surfaces treated with Cys-NgCAM (Fig. 14D,F). The neurons had a pseudounipolar morphology, usually seen in vivo with mature sensory neurons (Fig. 14F) compared to the multipolarity normally found in vitro.
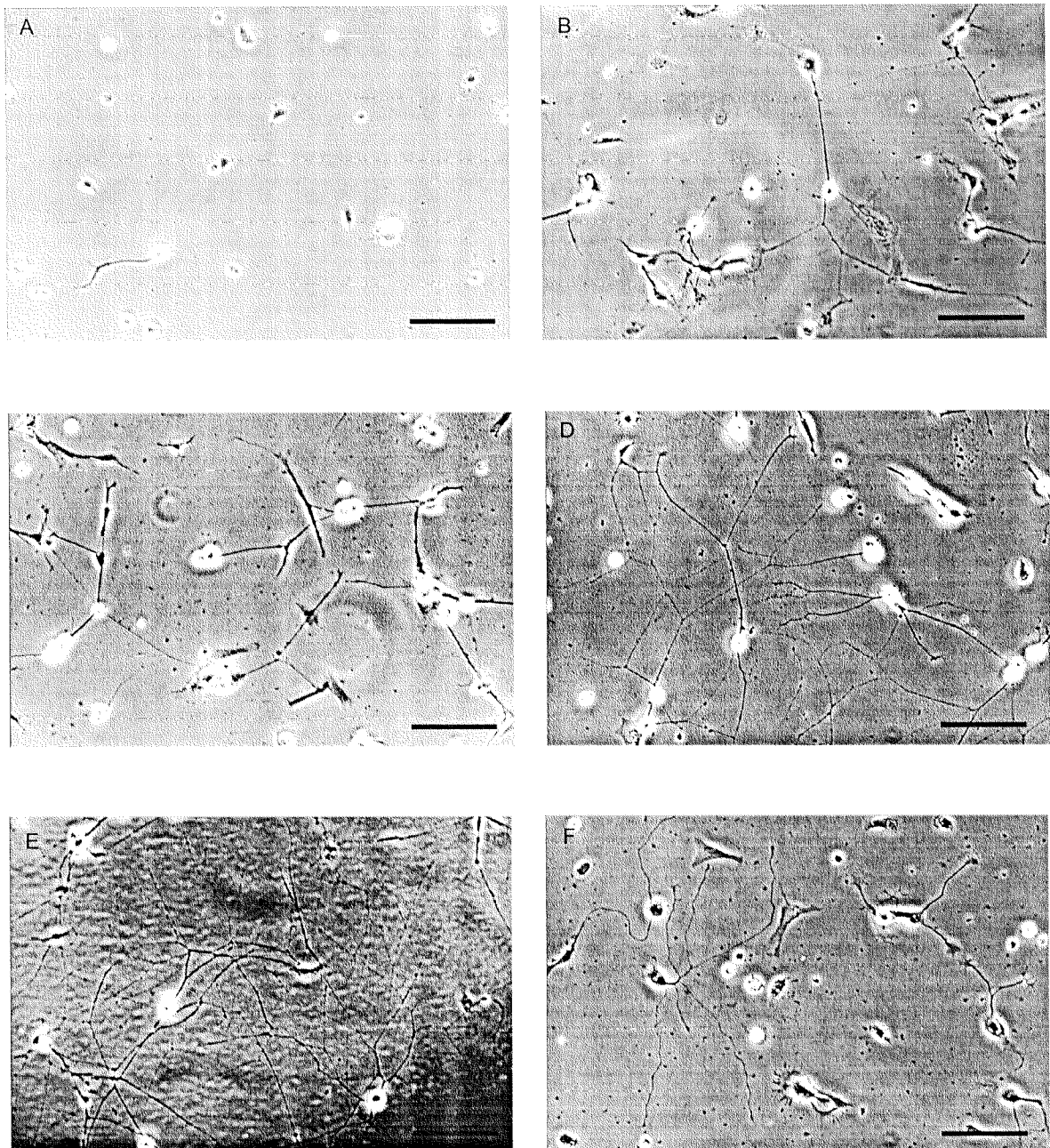
Figure 14: Dissociated DRG neurons on glass chips treated with different adhesion molecules

Cultures of dissociated chicken DRGs after 1 d in culture on APTES (A), RGDC (B), Cys-axonin-1 (C), Cys-NgCAM (D), laminin (E). (F) shows cell grown on Cys-NgCAM bound on gold surfaces. Note the monopolarity of the neurons. Scale bar 100 μm.

Table 3: Neurite outgrowth on different substrates

Substrate	Outgrowth (% of total cells)	Mean neurite length [μm] (n>30)
Aminosilane	20	40 ± 10
RGDC	60	124 ± 60
Laminin	90	n.d.
Cys-axonin-1	50	80 ± 30
Cys-NgCAM	80	231 ± 86

3.3.3   Long-term observation of cell cultures

If no attempts were made to inhibit division of non-neuronal cells glial cells and fibroblasts could be observed to form flat cell clusters after 5 days. After 1 week in culture these cells had formed a dense cell carpet on top of which neuron cells were growing (Fig. 15A).
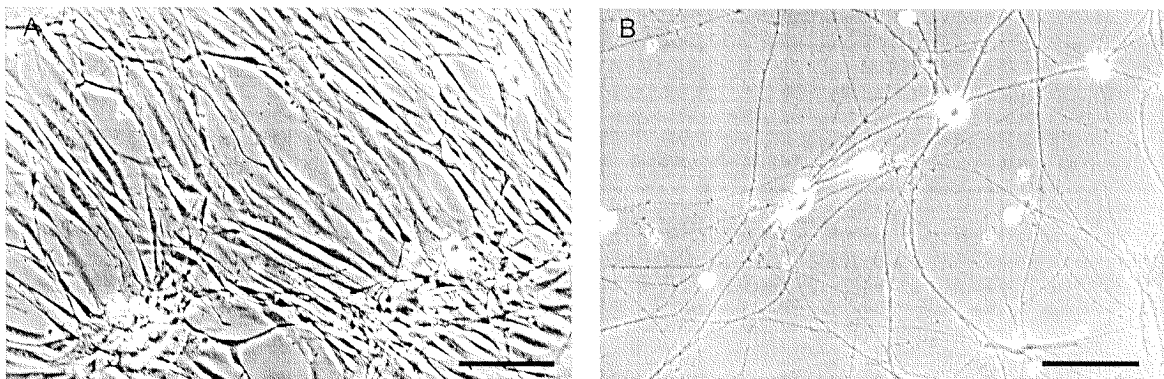

Figure 15: Long-term cultures of dissociated DRG neurons on RGDC
After 7 d in culture the non-neuronal cells proliferate and form a carpet of cells on which the neurons grow (A, on RGDC). If antimitotica are added to the medium, cell proliferation is inhibited (B, after 7 d on RGDC). Scale bar 100 μm.

Strong fasciculation of the neurites could be observed from day 3. These fascicles would form straight connection lines between the cells and even detach from the surface after a while. When antimitotica such as FUdR were added to the medium, after three weeks in culture nearly no non-neuronal cells were present in the culture. Neurite outgrowth in these cultures was comparable to the control without antimitotica in the cell medium (Fig. 15B).

3.3.4 Neurite outgrowth on patterns of cell adhesion molecules

Fluorescence labelled antibodies specific for the immobilised protein were used to visualise the formed protein patterns. However, as antibodies may bind selectively to some epitopes of the protein even when it is denatured, a successful binding was not a proof for the intact functionality of the protein. Patterns of Cys-axonin-1 were therefore created with both techniques, lift-off and etching, and used as substrates for neuron cultures (Fig. 16B). Much more neurites were found growing on patterns of the neural adhesion protein axonin-1 when the etching method was used to generate the pattern, indicating that the sucrose was effectively protecting this relatively large and sensitive protein. When using patterns of the short peptide RGDC (Fig. 16A), no such differences between lift-off and etching process could be observed . As RGDC has no tertiary structure that might be destroyed in the patterning processes the sucrose protection is not necessary. Varying the width of the protein lines from 5 to 25 μm a preference of the neurites to grow on narrow lines was observed. Pattern compliance was best on parallel lines smaller then 10 μm in width, followed by grid patterns with narrow adhesive lanes. After 5 d in culture the neurites started to fasciculate and did no longer follow the adhesive paths.
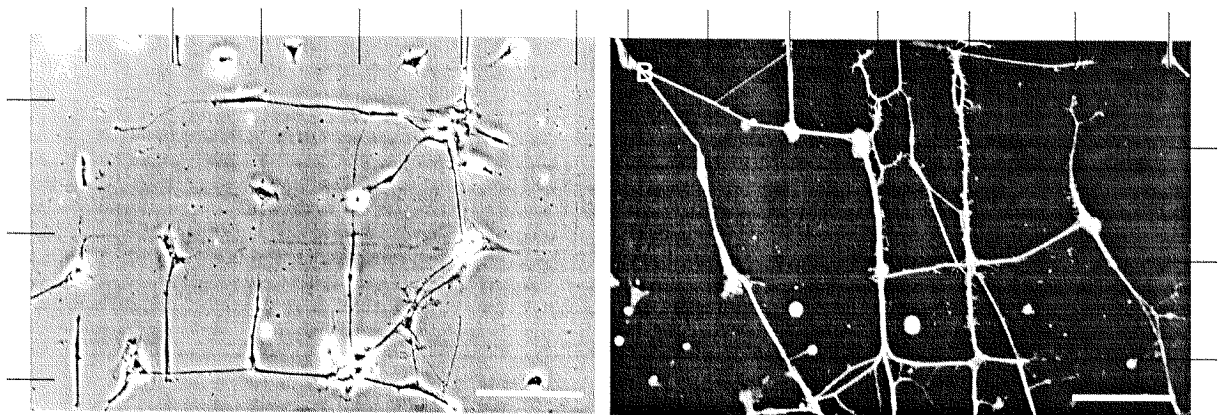

Figure 16: Neurite outgrowth on patterns of RGDC and Cys-axonin-1

Micrographs of DRGs cultured for 30 h on grid patterns of RGDC (A; 5 μm line width) and of Cys-axonin-1 (B; 15 μm line width). Patterns of RGDC were created using the lift-off method and patterns of Cys-axonin-1 were done with the etching method. The preparation in (B) was immunostained with FITC-labelled anti-axonin-1 antibody. Scale bar 100 μm

3.3.5   Reduction of non specific binding

A problem which is always encountered when working with proteins on surfaces is non specific binding of proteins. On gold surfaces as already mentioned this problem is prevented by the use of short chain thioalkanes. Experiments with immobilisation of Cys-axonin-1 on glass/polyimide half chips showed, that proteins bound also to the polyimide. Thus, cells seeded on the microstructured chips would form neurites not only in the microgrooves but also on the polyimide material. Therefore, a way to render the polyimide repellent to proteins and cells was examined. BSA and milk buffer could reduce adsorption of Cys-axonin-1 on the polyimide, but in combination with the immobilisation procedure (silanisation, crosslinker, protein) these substances could not be used. Another approach was to coat the polyimide surface with a hydrophobic silane (ODS). A flat PDMS stamp was wetted with ODS and stamped onto a microstructured chip. Because of the elevation of the polyimide above the glass and gold surfaces, the silane was bound only on top of the polyimide. Cells could no longer grow on the polyimide, whereas on the glass and gold parts of the chip perfect neurite outgrowth could be observed. Hydrophobic silanes were also used to prevent cell adhesion on glass substrates. Long chain alkane silanes, fluorinated silanes and PEG-derivatised surfaces have been shown to reduce cell attachment (Matsuzawa et al., 1997; Stenger et al., 1992; Branch et al., 2000) on patterned substrates. Indeed, poor or no cell attachment was observed on glass surfaces treated with these molecules (Fig. 17).

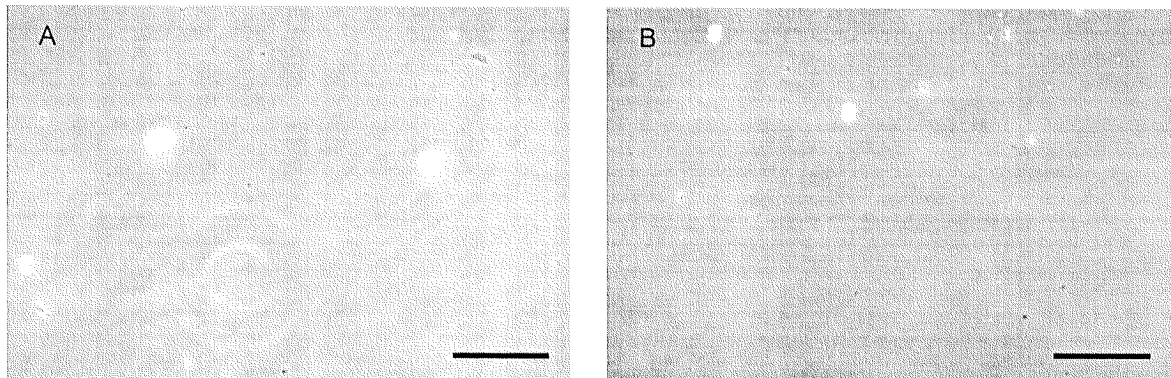**Figure 17: Hydrophobic surfaces suppress cell adhesion and neurite outgrowth**
Glass chips were treated with tridecafluoro-tetrahydrooctyl silane TFS (A) and octadecyltrichlorosilane ODS (B) and cells plated at a density of 5000 cells/cm^2 and cultured for 1 d. No neurite outgrowth was observed and the number of attached cells was significantly reduced as compared to glass treated with adhesion molecules. Scale bar 100 μm.

3.3.6 Positioning of cells into microgrooves

A tight cell-electrode contact is important for an efficient stimulation and recording of the neuron cells. The closer the cells are to the electrode the better the signals will transfer from the electrode to the cell and vice versa. Three ways of bringing the cells into the microgrooves contacted by gold electrodes were examined. As shown by Jimbo et al. (1993) a mask could be used to position cells into grooves of 150 µm side length. In a similar experiment the chip area was delimited by PDMS (0.5×5 mm) and cells were plated at a high density. However, no cell was found in a microgroove after 2 days of cultivation.

Positioning of single cells can also be achieved by laser tweezers or using micromanipulators (Townes-Anderson et al., 1998; Maher et al., 1999). In the laser tweezers setup cells are trapped in the focus of a laser beam and can be released at the position of interest. High numerical aperture objectives are required to generate the light trap (Svoboda and Block, 1994). However, due to the small depth of focus of such objectives this technique is not applicable with the used glass thickness (600 µm). Finally, positioning the cells with a micromanipulator was attempted. Glass pipettes with 30 to 50 µm inner diameter showed to be suitable for single cell placement into the microgrooves. An oil displacement handdriven micropump was used to suck the cells into the pipette and to release them into the microgrooves. This was very tedious work as the cells would jump out of the groove instead of settling down. Furthermore, the filling of all 25 grooves had to be accomplished within 20 min, the time required for cell attachment. Afterwards, the cells could only very hardly be sucked up with the micropipette and probably the cell membrane was damaged. However, whenever the placement had been successful, after 1 d in culture nearly all the cells had moved out of the grooves. Cells that were still in the groove had formed no neurites and were phase opaque indicating that they were apoptotic.

3.4 Discussion

In vivo the neural cell adhesion proteins axonin-1 and NgCAM are usually membrane bound proteins. With genetic engineering it is possible to modify the protein to allow secretion. An appropriate eukaryotic expression system has to be found as these proteins are glycosylated. Throughout expression, purification and finally covalent immobilisation the protein must retain its functionality. This was the case with both the engineered Cys-axonin-1 and Cys-NgCAM. However, the activity of the recombinant proteins in solution decreased slowly at 4 °C.

Published data on neurite outgrowth on axonin-1 and a homologue of NgCAM (L1/G4) adsorbed on culture dishes (Stoeckli et al., 1991) are slightly differing from the outgrowth observed when the proteins are covalently immobilised on the surface. The number of neurons with neurites is higher on adsorbed axonin-1 (80% vs. 50%), and the mean neurite

length is also longer (110 μm) compared to covalently bound Cys-axonin-1 (80 μm). These differences, as well as the longer mean neurite length on covalently bound Cys-NgCAM (230 μm vs. 150 μm on adsorbed L1/G4) are attributed to differences in surface coverage resulting from the coating technique.

The placement of the cells into the microgrooves showed to be more difficult than expected. It was possible to position the cells using a micromanipulator. However, after 1 day only the grooves were empty again. Even with high cell density coverage on the chip rarely a cell was found in the groove. The cells seemed to avoid these grooves. From these observations it was concluded that the size of the micogrooves (100 μm × 25 μm) was probably too small to accommodate these neuron cells (10–20 μm diameter). In a paper of Maher et al. (1999) a similar problem has been discussed. Inverted, truncated pyramidal holes of 30 μm side length and 16 μm depth, called neurowells, were fabricated to trap a single hippocampal cell. Tunnels for the outgrowing neurites leading away from the wells on the surface were designed to prevent cell body migration. The well dimensions however, seemed to be useful only for this cell type, as superior cervical ganglion cells escaped the wells after maturation. Finite-element analysis had suggested a cubic pit with 11 μm side length into which to place the cell for best results with extracellular electrodes recordings (Lind et al., 1991). The authors, however, do not make any comment on cell behaviour on such a narrow hole. Before a next generation design of the microchips is produced, the critical size parameters should be determined with in vitro experiments. An alternative method for the positioning of cells has been described (Martinoia et al., 1999; Müller et al., 1999). Both papers make use of microfluidics to direct cells to specified positions. While Martinoia and colleagues describe a simpler approach using laminar flow, in the work of Müller's group sophisticated elements such as funnel, aligner, cage and switch are presented to trap cells using negative dielectrophoresis.

Guided outgrowth of neurites could be observed on the photolithographically patterned cell adhesion molecules. Two simple layouts are presented: parallel lines and a grid pattern. Although alignment to the protein lanes was observed often, the cell bodies and neurites could also bridge areas where no protein was present. The line width of the adhesive area influenced neurite outgrowth. The narrower the protein lines the more neurites aligned to them. In order to avoid blurring of the cellular network definition after some days in vitro, coating the background areas with cell-repellent agents has been proposed (Branch et al., 2000). Exposing a stamped polylysine pattern to polyethylene glycol they created a pattern that would allow long-term cultures (29 days) of hippocampal pyramidal cells. The hydrophobic silanes ODS and TFS evaluated in this study are also suited to suppress growth of neurons on the background areas. The next step towards functional neural networks in vitro which will mimic networks in vivo (with signal propagation, processing, learning, etc.) is a logical network design which guides axons (output) to connect dendrites or cell bodies (input) of other cells. Wilkinson and Curtis (1999) propose a tile-based pattern. One tile has three cells, each with two inputs and one output (the axon) which splits in two. In this net-

work the signal can propagate in every direction and feedback loops are also possible. This network design implies that axonal/dendritic polarity can be induced in outgrowing neurons. Stenger et al. (1998) have shown that this is possible with a cross-shaped pattern of adhesive silane created with photolithographic techniques. Three arms of the cross consisted of an interrupted line, whereas the forth arm of the cross was a continuous line of adhesive silane. The discontinuities in the adhesive tracks were shown to induce dendritic growth, whereas an axon required the continuous adhesive path. A similar mechanism has been described by Esch et al. (1999). They cultured hippocampal neurons on alternating stripes of laminin and NgCAM and examined on which substrate the axon formed. They found that cells with their somata on laminin usually formed axons on NgCAM, whereas those with somata on NgCAM preferentially formed axons on laminin. This finding suggests that the *change* from one axon-promoting substrate to another provides a signal to induce the axon. This opens a wide field of surface modifications that could be used for the definition of neural networks. Not only adhesion promoting proteins can be immobilised on a surface, but also proteins with specific functions, such as induction of synapse formation, axon promotion, or specificity for a certain cell type. Culturing experiments with dissociated spinal cord neurons from mouse or chicken on Cys-axonin-1 and Cys-NgCAM functionalised glass surfaces failed. These neurons did not attach to the surface, formed clumps of cells and no neurite outgrowth could be observed. It seems therefore, that these proteins are neuron cell type specific. This can also be an advantage if co-cultures of different (neuron) cell types are desired.

Seite Leer /
Blank leaf

4

Cell-Surface Distance

4.1 Introduction

As outlined in the introduction (1.2) a tight sealing of the neuron cell membrane and the electrode surface is crucial for good S/N ratios. A better sealing means a close contact between the cell membrane and the electrode. In this project it is suggested that neural cell adhesion proteins immobilised on the surface could potentially reduce the cleft between membrane and electrode surface. In order to determine the distance between the cell membrane and the substrate surface, measurements with fluorescence interference contrast microscopy (FLIC) were performed in collaboration with Dieter Braun at the Max-Planck-Institute, München. FLIC-microscopy takes advantage of the interference of incident and reflected light above a mirror (Wiener effect). The standing modes of the electromagnetic field above the surface of silicon modulate the excitation and the emission of a fluorescent dye which is inserted in the cell membrane. The observed photons per unit time J_{fl} depend on the probabilities of excitation under stationary illumination (P_{ex}) and of emission into the detector (P_{em}) according to

$$J_{fl}(d_{ox}) = aP_{ex}(d_{ox}, d_{cleft})P_{em}(d_{ox}, d_{cleft}) + b$$

with a scaling factor a and a background b. For the calculation of the cell-substrate distance d_{cleft} an optical model with five layers (bulk silicon, oxide layer, extracellular cleft, cell membrane and cytoplasma) was assumed described by thickness and refractive index (Braun and Fromherz, 1997). Silicon chips with steps of different height of silicon oxide (d_{ox}) were produced. From the relative intensity of the cell membrane fluorescence on four different silicon oxide steps the cell-surface distance (d_{cleft}) can be calculated.

4.2 Methods

4.2.1   Neuron cell cultures on microstructured oxide chips

Silicon oxide chips (provided by D. Braun) were treated with cell adhesion molecules as described in section 3.2.1 and chicken DRG neurons were plated on the substrates as described in section 3.2.8.

The neuron cell membranes were stained 20 h after seeding with the amphiphilic dye 1,1'-didodecyl-3,3,3',3'-tetramethylindocarbocyanine perchlorate ($DiIC_{12}$, Molecular Probes). A 5 mM $DiIC_{12}$ stock solution in ethanol was diluted 1:1000 in PBS- resulting in a suspension of dye aggregates. The cell medium was removed and substituted with 3 ml of the dye solution. The dye was added, removed and re-added carefully to the cells, in order to enhance staining. After 5 min at 37 °C this procedure was repeated once. The living cells were kept in PBS- during observation with the fluorescence microscope. For the FLIC measurements two independent cell culture preparation and two chips per coating were examined.

4.2.2   Determination of cell-surface distance

Theory and set-up used for the calculation of the cell-surface distance with fluorescence interference contrast microscopy have been described by Lambacher and Fromherz (1996) and Braun and Fromherz (1997). Briefly, fluorescence pictures (Fig. 18) were taken through a water immersion objective (100×, numerical aperture 1.0, Zeiss Axioskop) with opened Abbe condenser at 546 nm excitation wavelength. Emitted light was filtered and detected between 580 and 640 nm with a CCD-camera (Sony chip ICX039AL, HRX, Theta Systems, Germany) which had an effective pixel size of 90×90 nm. Exposure times varied between 40 and 320 ms. In order to identify the oxide squares below the cell a reference picture was made through the same objective filtering light from a halogen lamp at 630 nm and with closed Abbe condenser (Fig. 18D). Pictures taken with open Abbe condenser showed no intensity contrast coming from the cells. On each oxide square regions of equal fluorescence intensity were defined and fitted by the mentioned optical theory of interference. Minimal distances of single cells were determined and averaged for each substrate.

4.3 Results

4.3.1 Cell membrane-surface distances

Areas of homogeneous fluorescence intensity were defined (Fig. 18C) and the averaged
intensities were plotted versus the oxide square thickness (Fig. 19). For the regions r1–r4
defined in Fig. 18C the lowest intensity was on the thinnest oxide, indicating a narrow cleft
(Fig.19A), whereas in the regions R1–R4 of Fig. 18C the intensity was highest on the thin-
nest oxide indicative of a large cell-surface distance, as the standing modes have a node near
silicon (Fig. 19B). The distance values were fitted with the distance curve calculation pro-
gram developed by D. Braun (Fig. 19, solid lines; http://mnphys.biochem.mpg.de/
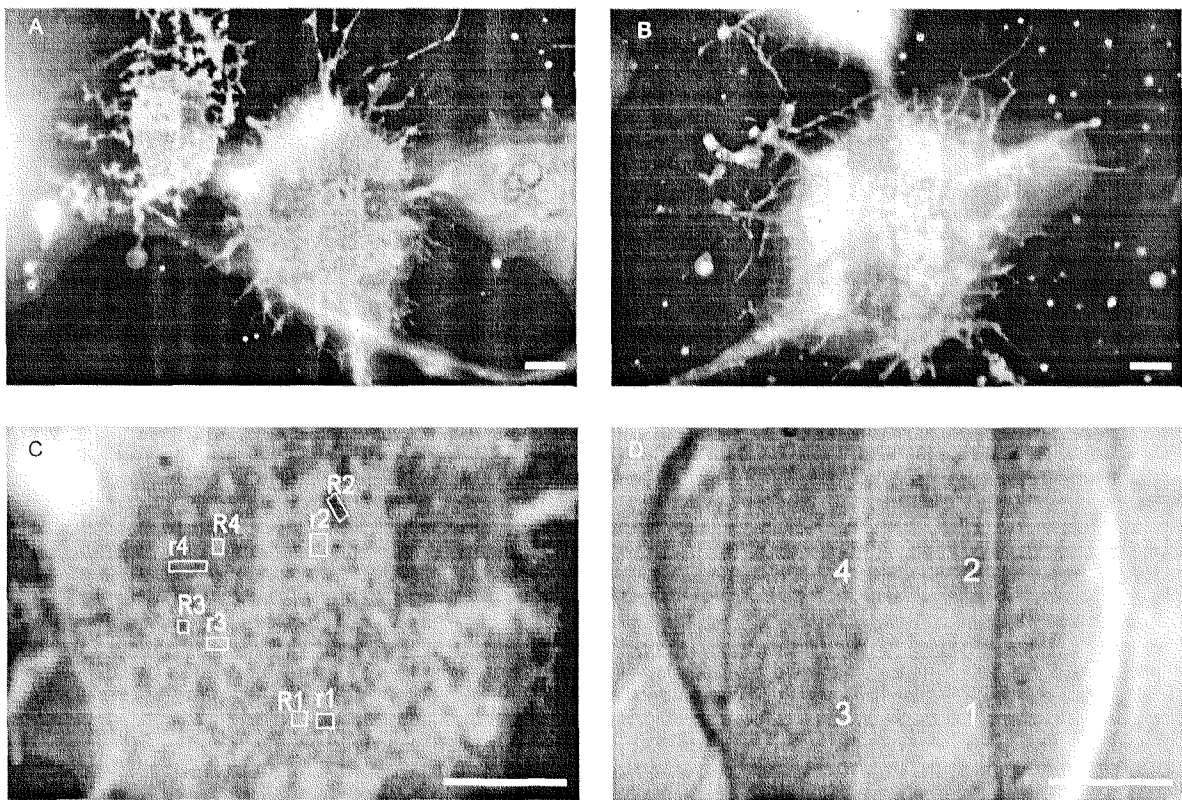projects/flic/flic_root.html) .

Figure 18: Fluorescence micrographs of neurons cultured on silicon oxide chips
Fluorescence micrographs of DRG neurons cultured 20 h on APTES (A) and axonin-1 (B). (C) shows
a detailed view of the cell in the centre of (A). Fluorescence intensities were measured over the
regions delimited by white boxes (r1-r4 and R1-R4 in (C)) and the correspondent oxide thickness
assigned comparing with the picture of the cell at the same position made with closed Abbe con-
denser in white light (D). Oxide thickness 1-4 in (D) correspond to 10, 55, 110 and 155 nm, respec-
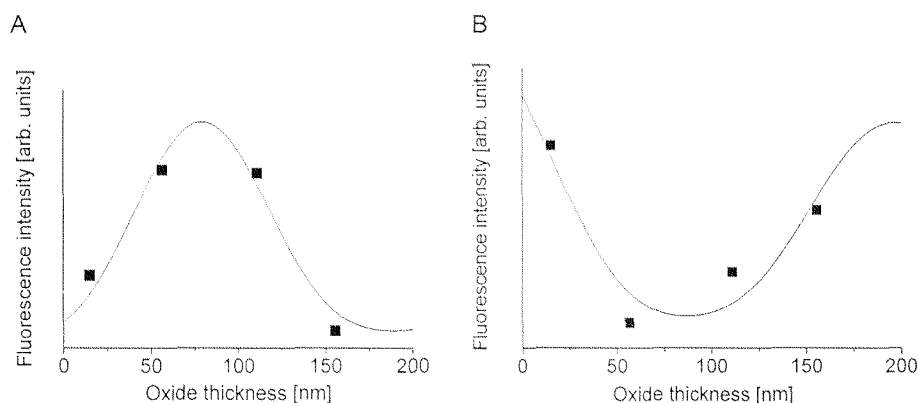tively. Scale bars 5 μm.

Figure 19: Determination of the minimum and maximum cell-surface distances
The average fluorescence intensities of boxes r1-r4 (A) and R1-R4 (B) of Fig. 18C were plotted vs. the four different oxide thickness (■). The curve was fitted with the distance calculation program (see text). The calculated distances were 34 ± 5 nm for (A) and 154 ± 7 nm for (B).

As it can be seen in Fig. 18 the fluorescence intensity is not homogeneously distributed over the whole oxide square area, rather it shows an irregular, dotted pattern. Analysing the cell-surface distance these membrane patches revealed differences from 30 to 100 nm (Fig. 19).This phenomenon was observed on all substrates and has been mentioned by Braun and Fromherz (1998) for rat neuron cultures on chips with adsorbed polylysine. For the calculation of the minimal cell-surface distance for each substrate type only the smallest distance value of every cell was taken.

The results are summarized in Table 4.

Table 4: Minimal cell-surface distances as determined by FLIC

Substrate	Measured cell-surface distance [nm]	Theoretical molecule length [nm]
APTES	39 ± 3	1-2
RGDC	39 ± 4	2-3
Cys-axonin-1	37 ± 10	32
Cys-NgCAM	47 ± 8	44
Laminin	91 ± 4	113
Polylysine	54 ± 9	?

The closest cell-surface contact was found on the Cys-axonin-1 substrate (37 ± 10 nm, n = 16) and on the APTES surface (39 ± 3 nm, n = 7). On Cys-NgCAM substrate a longer distance was determined (47 ± 8 nm, n = 14), whereas on the polylysine substrate the minimal distance was found to be 54 ± 9 nm (n = 7). The cleft separating the cell membrane grown on laminin from the surface (91 ± 4 nm, n = 7) was much wider and comparable to the previously reported value for hippocampal cells of 104 ± 1 nm (Braun and Fromherz, 1998). On chips treated with the short adhesion peptide RGDC the cell-surface distances were non-uniform. A cluster for cells with a mean distance of 39 ± 4 nm (n = 5) can be defined (Fig. 6, dashed line), whereas the distance of the further cells ranged between 80 and 160 nm.
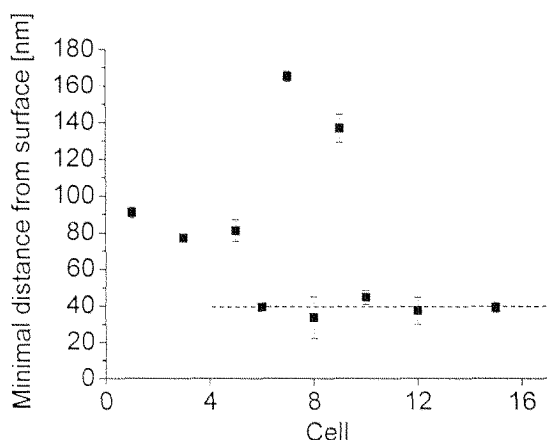

Figure 20: Calculated minimal distances from all cells measured on RGDC-treated chips

Cell surface distances of 15 cells were calculated and plotted vs. the cell number. Low values are clustered in a mean cell-substrate distance of 39 nm (dashed line).

4.4 Discussion

From early experiments with dissociated neuron cultures it was recognised that a positively charged surface promotes adhesion of neurons (Yavin and Yavin, 1974; Letourneau, 1975). Presently, the positively charged polyamino acids polyornithine and polylysine are well established as coating molecules for culture dishes. The exact nature of the attachment mechanism to these surfaces is not yet clear. However, it seems widely accepted, that negatively charged proteoglycans or lipids of the cell membrane could interact with the surface-

bound polycations (Yavin and Yavin, 1974; McKeehan and Ham, 1976; Glass et al., 1994). The assumption that a positive charge is sufficient for cell adhesion was refined by Kleinfeld et al., 1988). They postulate that the chemical structure may additionally be important as indicated by the finding that di-amino terminated molecules on surfaces were more potent adhesion promoters than surfaces treated with mono-amino molecules. This is in agreement with our observation that cells are growing poorly on the mono-amino silane APTES. The distance of the cell membrane to the substrate on APTES is at a minimum. Adhesion mechanism of cells on APTES and polylysine is probably comparable. The measured cell-surface distance, however, is larger on polylysine (54 nm). Polylysine which is physisorbed onto the chip surface is more extended than the short-chain APTES and the coating is not as stable as the covalently bound APTES, probably resulting in an increased mean distance value. Fig. 21 shows estimated lengths of the adhesion molecules used in this study.
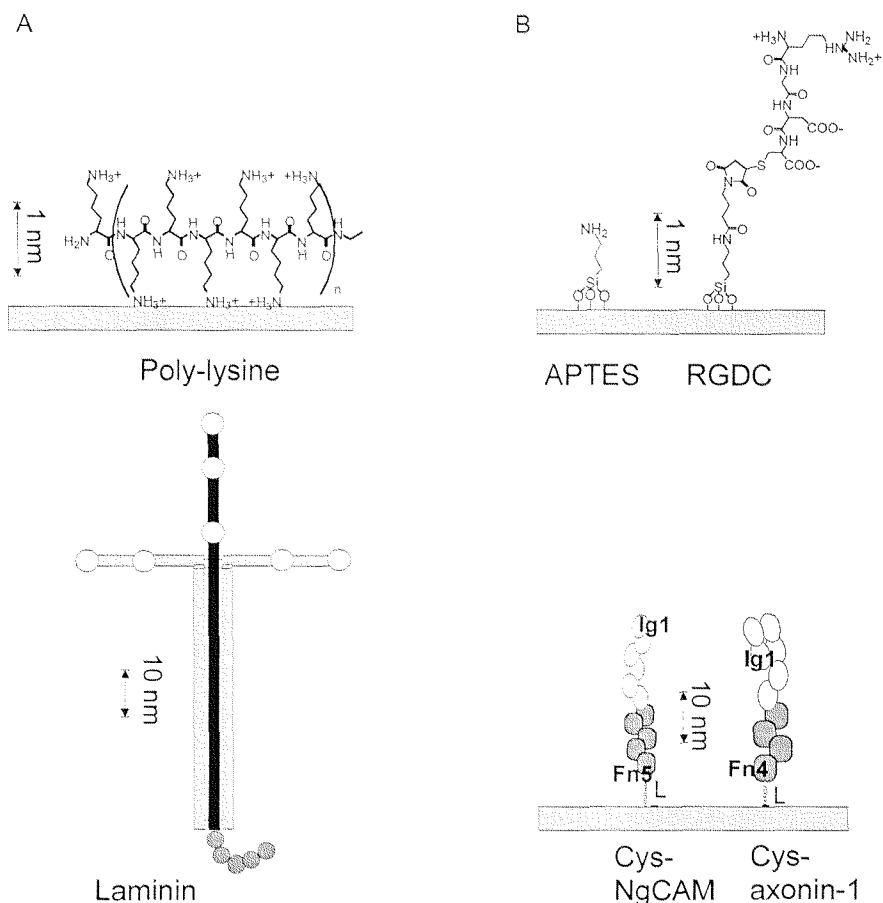

Figure 21: Theoretical length of adhesion molecules

Polylysine and laminin were immobilised by physisorption (A). APTES, RGDC, Cys-axonin-1 and Cys-NgCAM were covalently immobilised on the oxide via silane chemistry with a crosslinker molecule for an oriented immobilisation (B). (L: peptide linker with C-terminal cysteine, crosslinker and amino-silane. Ig: immunoglobulin-like domain. Fn: fibronectin-like domain).

In contrast to APTES and polylysine, the other adhesion molecules studied bind cells specifically via receptor molecules. The extracellular matrix protein laminin is recognized by integrin molecules present in the cell membrane (McKerracher et al., 1996). The integrins are a family of receptor proteins consisting of heterodimers of distinct α and β chains which protrude 20–22 nm into the extracellular space (Nermut et al., 1988). Neurons cultured on laminin coated chips are separated from the surface by a rather wide cleft of 91 nm as it can be expected considering the dimensions of laminin (72×113 nm; Engel et al., 1981). Braun and Fromherz (1998) have reported a homogeneous 104 nm thick cleft for rat neuron cultures on adsorbed laminin. A cleft of this width will result in a loose sealing to extracellular electrodes. Some of the cell adhesion functions of laminin are mimicked by the short peptide sequence RGD that is recognized by different integrins (Glass et al., 1994; Burridge and Chrzanowska-Wodnicka, 1996). A theoretical distance of 25 nm can be assumed by adding the dimension of the RGDC covalently immobilized on the surface (2–3 nm) and the mentioned length of the integrin molecule protruding form the cell membrane (20–22 nm). The actual determined distance was slightly larger (39 nm), because, the glycocalyx of the cell may limit the minimum distance value (as discussed below). It is not clear, why longer distances for cells on RGDC chips were found in some cases. Further receptor molecules may be involved or different neuron subtypes were observed. Since this phenomenon was not observed with other adhesion molecules a methodical fault can be excluded.

Several studies have been performed to elucidate the interactions of axonin-1 and NgCAM with other cell adhesion proteins. Although a homophilic binding of axonin-1 between two cells could be shown with heterologous expression on myeloma cells (Rader et al., 1993) and in crystal structure studies (Freigang et al., 2000), the biological function of this complex is not yet clear. Neurite outgrowth on axonin-1 substrates is probably mediated by NrCAM (Suter et al., 1995; Lustig et al., 1999) whereas neurite outgrowth on NgCAM substrates is thought to be mediated by the tetrameric (axonin-1/NgCAM)$_2$ complex. Considering that an Ig-domain is about 4 nm long (Schiffer et al., 1973) and assuming similar dimensions for the fibronectin-like domains, the length of the immobilized Cys-axonin-1 would be 32 nm, and Cys-NgCAM is estimated to be 44 nm long. From the structural models of interactions we would expect that the cleft between cell and these substrates should be in the range of 50–70 nm. The cell-surface distances measured by FLIC confirm these expectations. On Cys-axonin-1 substrate the cells are at a minimum distance (37 nm) and slightly more distant on Cys-NgCAM-treated surfaces (47 nm).

The fact that no cell-surface distance below 35 nm was found for DRG neurons cultured on different substrates indicates that additional bulky molecules may be present. It is known, that cells are coated with a carbohydrate-rich layer, the so-called glycocalyx. Early electron microscopy works on chicken DRGs had revealed the existence of a cell coat on these neurons (James and Tresman, 1972). Depending on the staining method the thickness of the cell coats measured varied from 30 nm (ruthenium red staining) to 120 nm (lanthanum permanganate staining). The glycocalyx of red blood cells has been estimated to be

only 6 nm thick (Linss et al., 1991). Indeed, red blood cell ghosts adhered to polylysine coated surfaces at a very low distance of 12 nm as determined using FLIC microscopy (Braun and Fromherz, 1997). We thus conclude that the glycocalyx may prevent a closer contact of the cell membrane to the surface by steric hindrance. Therefore, we postulate that 35–40 nm is the minimum cell-surface distance for DRG neurons. Whether this is sufficient to improve the signal-to-noise ratio in electrophysiological experiments with extracellular electrodes has to be shown. Form the simulations made by Grattarola and colleagues (Grattarola et al., 1991) with the SPICE program at a cell-surface distance of 50 nm the recorded signal is expected to be in the range of 800 µV. Reducing the distance to 20 nm would give a signal in the range of 2–3 mV. With the measured gap of about 40 nm on Cys-axonin-1 signals in the 1 mV range can therefore be expected. Additionally, the glia cells continue to proliferate in culture and eventually form a dense glia carpet on *top* of which the neurons grow. Therefore, after a week or two the distance from neuron cell membrane to electrode surface will be a cell layer of glia. Attempts to solve this problem using co-culture systems have been reported by several groups. Kleinfeld (Kleinfeld et al., 1988) reported the creation of an unpatterned area for feeder cells surrounding the patterned neurons. Another group (Maher et al., 1999) seeded glia cells on a coverslip and laid it upside down 2 mm above the electrode array chip. The secretions of the glia would diffuse into the cell medium and be available for the neurons.

Neurons have been reported to adhere to the surface in so called point contacts (Streeter and Rees, 1987; Arregui et al., 1994), i.e. small (90–200 nm) regions of the membrane closely apposed to the substrate, in which other types of integrins and cytoskeletal anchor proteins than those found in focal contacts are involved (Tawil et al., 1993; Arregui et al., 1994). Note the irregular dotted pattern of the membrane in the fluorescence images of the cells (Fig. 18). Patches of membrane appear darker than other areas indicating that some parts of the membrane are more distant from the surface than others (Fig. 18C and Fig. 19). The difference between the distances of these patches was in the range of 30–100 nm for most cells. The lateral dimensions of these dots ranged from 100 to 500 nm, but sometimes they were even larger than 1 µm. Thus, the observed dots may represent point contacts. Identification of the involved proteins by using immunocytochemical methods could help to confirm this assumption. The determined cell-surface distances are *mean* values over the determined areas. The lateral resolution of the FLIC technique is in the range of a few hundred nanometers. It is possible, that within these membrane patches the cell membrane has points of closer contact to the surface, that cannot be resolved with this technique.

5

Stimulation and Recording

5.1 Introduction

Extracellular recordings from neural cells can be performed measuring the potential difference between the extracellular electrode and ground (Grattarola et al., 1997; Gross et al., 1997b; Maher et al., 1999), or between a pair of electrodes (Breckenridge et al., 1995; Maeda et al., 1995). In general, the recorded signal is amplified by high impedance amplifiers and filtered to cut off unwanted low and high frequencies, the band width being between 0 Hz–20 kHz. The signal is then digitised in the data acquisition board at a resolution of typically 12 or 16 bit. Finally, a software is used for data processing and analysis. A typical workstation for MEA recording is shown in Fig. 22.
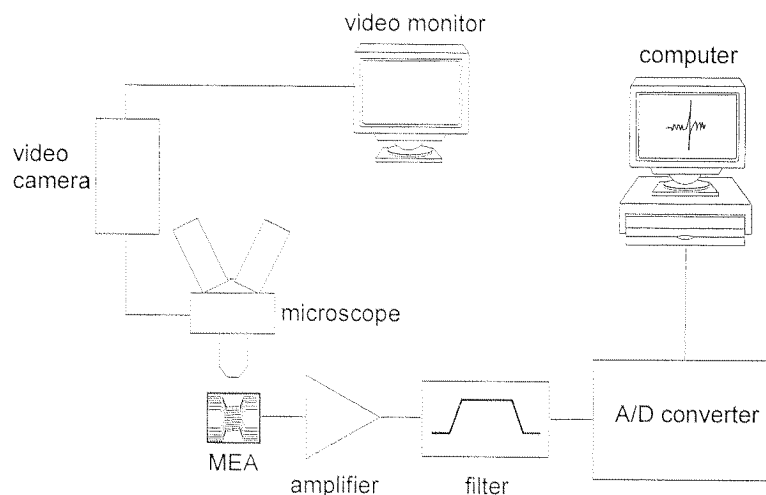
Figure 22: Sketch of a workstation for signal recording from multielectrode arrays

The extracellular electrodes on the MEA-chip are connected to amplifier and filtering units. The recorded signal is digitised and analysed with a computer. The cells can be observed with a microscope or on a video system connected to the microscope while recording.

A number of groups have started to integrate the amplifying and filtering units in the direct vicinity of the chip in order to reduce noise. Pancrazio et al. (1998) have described a CMOS amplifier-based system with measurement and stimulation capability which is connected directly to the multielectrode array chip via zebra strips. Commercially available electrode array systems offer also filtering and amplifier systems to which the chip is connected directly and which can be mounted on the microscope stage (Multichannelsystems, Reutlingen, Germany; Matsuhita Electric Industrial Co., Panasonic, Kyoto, Japan). These vendors offer whole packages with chips, signal processing units and data analysis software.

For stimulation of neurons via extracellular electrodes current pulses in the 100 nA range are applied (Regehr et al., 1988; Wilson et al., 1994). In order to improve S/N-ratios the impedance of these electrodes is reduced by electroplatinisation resulting in impedances ranging between 200 kΩ and 1 MΩ (Wilson et al., 1994; Breckenridge et al., 1995; Maher et al., 1999). Furthermore, the voltage at the electrode-medium interface must not exceed 1 V to avoid damaging the electrode material and the cells. The applied stimulus pulses have a duration between 300 µs and a few tens of milliseconds. Many groups have recorded extracellular and intracellular signals in parallel to control the performance of the extracellular electrode (Jimbo et al., 1993; Wilson et al., 1994; Breckenridge et al., 1995).

The results presented here should be seen as preliminary. The primary aim was to investigate if it is possible to culture cells on the chip embedded in the circuit board, if these cultured cells were electrically active and finally, if it was possible to apply current pulses through the gold electrodes. The effect of the extracellular stimulation was monitored with an intracellular electrode in whole cell recording mode.

5.2   Methods

5.2.1   Preparation of the microstructured chip

The experiments described in this chapter were performed with the microstructured chip bonded to a printed circuit board as described in 2.2.3. Fig. 23 shows a microstructured silicon nitride type chip which was glued on a printed circuit board. The reason for using these chips were twofold: First, the polyimide layer depolarised the light in differential interference contrast microscopy used in the recording setup. This interference overpowered the interference caused by the cell membranes by many times and as a consequence the cells could not be seen. Second, the positioning problems, as discussed, could be circumvented with the thin silicon nitride layer (400 nm). Bond wires connect the chip to the circuit board. A small glass ring glued on the chip before functionalisation with RGDC served as cell culturing chamber (arrowhead in Fig. 23). A second ring with 2 cm diameter and 3 mm height was glued on the printed circuit board (Fig. 23, white circle). The small glass ring was
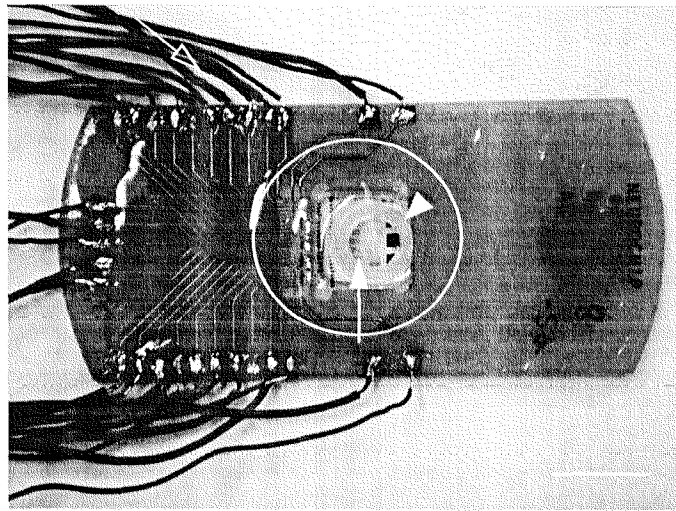
Figure 23: Chip bonded into printed circuit board used for electrophysiology experiments

A silicon nitride-type chip was glued into the chip holder. Contact pads on the chip were wire bonded to contacts on the board. Wires for connection to the stimulus generator were soldered on the board (open arrow). A small glass ring (white arrow head) was glued on the chip and the board embedded with PDMS. A second glass ring (white ring) was glued on the board for patch clamp experiments. The white arrow indicates the position of the microgrooves. Scale bar 10 mm.

removed before the chip was mounted on the holder on the microscope stage for intracellular recordings. The second ring then served as medium containing chamber.

The experiments were done with 4–7 d old cultures of dissociated DRGs plated at high density on chips functionalised with RGDC as described in section 3.2.8.

5.2.2   Measurement setup

These experiments were performed in the lab of Dr. Christian Stricker (Institute of Neuroinformatics, Zürich). The chip with the cell culture was mounted within a custom made holder on a stage. Immediately, medium was perfused through the cell chamber at a flow rate of ca. 5 ml/min. The pH of the medium was controlled in the bottle with constant 95% O_2 and 5% CO_2 bubbling. A water-jacket (Grant-Instruments FH15V, Cambridge, UK) was used to warm the medium to 35 ± 1 °C. The microscope (Axioskop FS, Zeiss; 40× water immersion objective) was equipped with a digital camera (Hamamatsu C2400-ER) which allowed infrared imaging based on a polarizer and an IR-filter (IR-DIC; Omega-optical filter 740–800 nm bandpass). The micropipette positioning was monitored on a high resolution video monitor (Sony PVM96E).

Micropipettes (borosilicate glass; 1 mm inner-, 2 mm outer-diameter; Hilgenberg glass, Germany) with an inner tip diameter of about 3 μm and 3–5 MΩ resistance were pulled by a 4-stage pull with an automatic puller (P-97, Sutter Instruments, USA). The pipette was filled with intracellular solution (see below) and mounted on a holder (headstage HS-2A, 0.1 gain, Axon Instruments, USA) fixed on a mechanical manipulator (design JCSMR-ANU[1], Canberra, Australia). The junction potential (-11 mV) was not subtracted. Stimulation and recording via the patch pipette were done with an Axioclamp 2B (Axon Instruments, USA) and a sample and hold amplifier (8 pole bessel, design JCSMR-ANU, Canberra, Australia). Data acquisition was controlled via a ITC-18 board connected to a PowerMac (Apple). Data were filtered at 20 kHz and sampled at 10 kHz. For the stimulation via the extracellular electrodes the contacting wire was connected to a stimulus generator (Stimulator-II, Axon Instruments, USA).

Intracellular solution for patch clamp:

2256 mg	D-Gluconic acid (Sigma G-4500); f. c.[a] 115 mM	
119 mg	KCl (Sigma P-4504); f. c. 20 mM	
128 mg	HEPES (Sigma H-0891); f. c. 10 mM	
101 mg	Phospho-Kreatine (Sigma P-6915); f. c. 10 mM	
8 mg	Mg-ATP (Sigma A-9187); f. c. 4 mM	
499 mg	Biocytin (Sigma B-1758); f. c. 0.3 mM	
	to 50 ml with H_2O, osmolarity adjusted to 303 mOsm at pH 7.3 (KOH or HCl)	

a. f.c.: final concentration

5.2.3   Stimulation through gold electrodes and intracellular recording

Neuron cells on or near gold electrodes and with a healthy looking cell membrane (smooth surface, no inclusion, diameter ~15 μm, spheric shape) were chosen. Cell viability was tested by stimulating and recording in whole cell recording mode. Measurements of action potentials in current clamp and of action currents in voltage clamp were performed. If the cell showed active responses a stimulus current was applied with the extracellular gold electrode starting from 50 μA/20 μs pulse duration until an action potential/current could be detected with the intracellular electrode. The transient of the stimulus artefact was an order of magnitude faster than that of the cell itself. Therefore, the two could be distinguished.

---

1. John Curtin School of Medical Research, Australian National University

5.3 Results

5.3.1 Cell cultures on microstructured chips

In a first simplified experimental setup the nearly planar silicon nitride-type chips were used for cell culturing. Culturing of neurons within the microgrooves turned out to be difficult with the groove dimensions present on the microstructured chip with the polyimide. Therefore, it was decided to substitute the polyimide layer by silicon nitride as second insulating layer.

Initially, neurons were seeded at low densities, however, due to the poor covering of electrodes with cells the plating density was increased. The morphology of the neurons was the same as on unstructured surfaces. The microscope on the recording rig was equipped with filters for infrared differential interference contrast microscopy. This method allowed to view the cultures in a 3-dimensional way. The inspection revealed that even at low cell density the cells do not grow straight on the substrate. On the contrary, there seems to be a layer of material (cell debris, cell secreted matrix) on top of which the cells are growing. Cells growing over the microgrooves, which on these chips had a depth of ca. 600 nm, did not make any (observable) contact with the groove ground below (glass or gold).

5.3.2 Intracellular stimulation and recording

The resting potential of DRG neurons was about -60 mV in these cultures. Action currents in the nA range were elicited in voltage clamp mode upon voltage jumps of +(20–30) mV. Action potentials were elicited by an intracellular current of 0.05–0.2 nA. Repetitive firing could be observed in some cells. Glia cells could be clearly distinguished by the rectifying currents after stimulation and lack of action potential generation. Fig. 24 shows a typical action potential recorded from a DRG neuron. The action potential in these cultures had a mean amplitude of 89 ± 13 mV (n = 36) and the mean duration at half amplitude was 3,3 ± 1.6 ms (n = 36).

5.3.3 Extracellular stimulation and intracellular recording

If action currents and action potentials could be recorded in whole cell patch mode, the extracellular gold electrode lying near the cell was connected to the stimulus pulse generator. Successful stimulation could be recorded with intracellular electrodes on a few occasions. In Fig. 25B one such recording is shown. An action potential was recorded with the intracellular electrode when current pulses of 150 μA/100 μs were applied through the extracel-
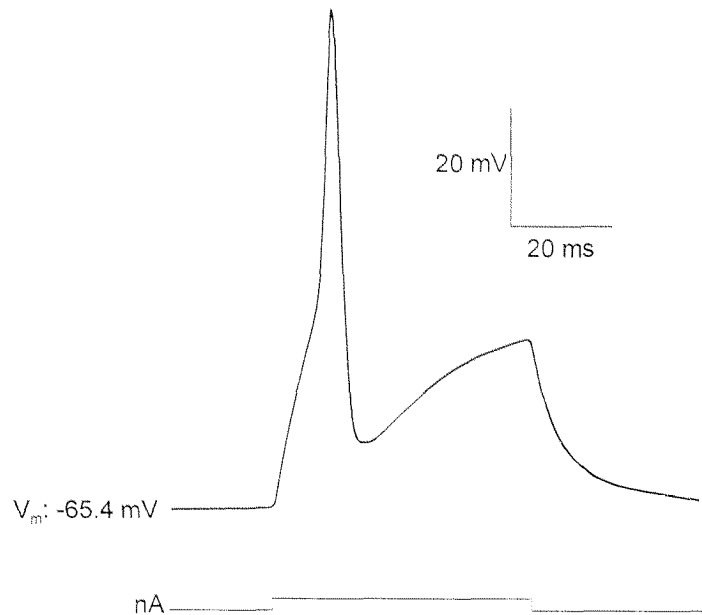
Figure 24: Action potential recorded in whole cell recording
The neuron (the same as shown in Fig. 25) was intracellularly stimulated in current clamp mode with
30 ms pulses of 0.1 nA through the glass microelectrode. The current trace is shown below the curve.
The action potential was recorded with the same electrode and had an amplitude of 96 mV and the
duration at half-amplitude was 3.1 ms.

lular gold electrode on the cell in Fig. 25A. The mean amplitude of the recorded action
potentials was 75 ± 18 mV (n = 11) and the mean duration at half-amplitude was
3.7 ± 1.3 ms (n = 11). The action potential recorded after stimulation with surface elec-
trodes is therefore not significantly different from the one recorded after intracellular stim-
ulation. However, if the graphs in Fig. 24 and Fig. 25B are compared the depolarisation
phase of the intracellularly elicited action potential seems to bee slower than in the case of
the extracellular stimulation. This is due to the different duration of the stimulus pulses. The
intracellular stimulation is about two orders of magnitude slower than the extracellular one.
What can be seen as a 'shoulder' in the depolarisation phase in Fig. 24 is part of the charging
curve of the cell membrane. The very fast current pulses through the extracellular electrodes
can depolarise the cell membrane much faster.

Often the extracellular stimulation of the neuron failed. Several reasons could lead to this
failure: If the neuron was not close enough to the surface gold electrode, a very large part
of the stimulation current dissipated into the surrounding medium and did not reach the
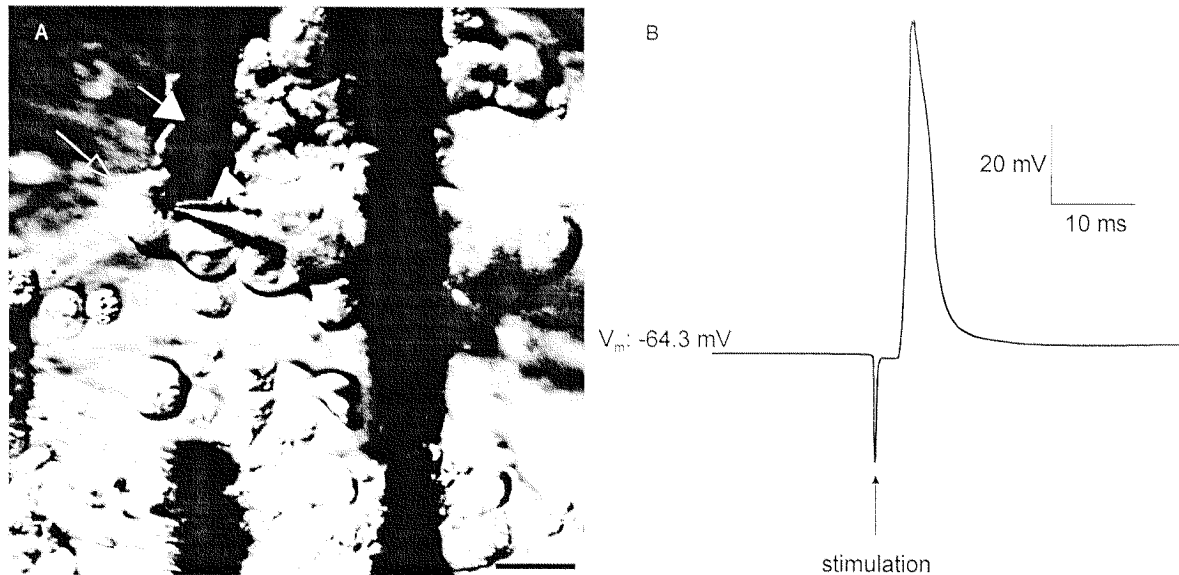cell. Application of stimulation currents higher than 400 µA led to bubble formation at the

Figure 25: Action potential stimulated extracellularly and recorded intracellularly

(A) IR-DIC micrograph of DRG neurons cultured on the extracellular electrode array. The extracellular electrode (arrow) close to the neuron cell (open arrow) stimulates the cell with a current pulse of 150 μA during 100 μs. A micropipette attached to the neuron served as recording electrode (white arrowhead). The size of the gold lanes was 25 μm. Scale bar 20 μm. (B) Action potential recorded with the intracellular electrode after extracellular stimulation (amplitude 88 mV, duration 3.0 ms).

electrode surface indicating that electrochemical reactions were occurring. The gold electrodes were damaged afterwards, at sites of bubble formation the gold was 'evaporated'. Additionally, if the applied current pulse was too large, the electrode seal would become leaky. Probably the cell membrane was damaged by the current, i. e. the heat produced by the pulse. Furthermore, with increasing number of recyclings of the chip the cell cultures were more and more difficult to grow. The cells adhered only poorly to the surface and after a few days in culture they were apoptotic. The cleaning procedure described in 2.2.3 (detergent and acid) could restore the chip surface only for a few times. Furthermore, the insulating silicon nitride and silicon oxide layers were damaged with time. Most often these defects were observed above gold lanes. Applied currents would therefore leak out into the medium before reaching the electrode.

5.4 Discussion

These preliminary electrophysiological experiments demonstrate that the microstructured chip can be used for stimulation of single neurons. The neurons grow on these chips as they do on unstructured surfaces and are electrically active. The action potential amplitude and width are comparable to published values for cultured DRGs stimulated and recorded intracellularly (Dichter and Fischbach, 1977).

Due to the difficulties that arose in the course of the experiments with chip recycling and the resulting short life time of the chip, it was not possible to use the surface electrodes for *recording* cell activity. However, there is no reason why this should not be feasible, although nothing can be said about the quality of the recorded signal.

The IR-DIC microscopy allowed to make interesting observations concerning the cell cultures. In cultures that are a few days old the cells do not grow straight on the surface. There seemed to be a layer of material between the chip surface and the bottom of the cell. The cell-surface distances measured with FLIC microscopy (chapter 4) were done after 20–24 h in culture. The electrophysiological experiments were performed on 4–7 d old cultures. It is known that cells produce extracellular matrix in culture. This could be the reason for the observed layer of material laying between cell surface and neuron cell membrane. The thickness of this layer was a few micrometers. The glia carpet observed after 5 days in culture (chapter 3) can additionally increase the gap between electrode and neurons. It is not clear what role the immobilised cell adhesion proteins that reduce the cell-surface distance will play in this context. However, it can be said that this cell and material layers do not prevent the current transfer from the neuron cell membrane to the surface electrode, as successful recordings of other groups on several months old cultures showed (Gross et al., 1995). They recorded signals in the range of a few hundred microvolts (S/N-ratio 5:1).

An interesting issue that has been found by Vassanelli and Fromherz (1999) and discussed by Wilkinson and Curtis (1999) is the distribution of the ion channels in the neuron cell membrane. In rat hippocampal neurons cultured on FET devices the voltage-gated channels responsible for the A-type and K-type potassium conductances were distributed inhomogeneously in the cell membrane. The K-type channels were preferentially located in the adhesion region (cell bottom) and the A-type channels in the membrane part not in contact with the surface (top of the cell). This channel segregation affects the size and shape of the recorded signal (Vassanelli and Fromherz, 1999). For further studies it will therefore be of interest to investigate where the best position of the extracellular electrode is.

6

Summary and Outlook

6.1 Summary of results

Starting from the working hypothesis the work was divided in several parts. The most important achievements of the project can be summarised as follows:

- The produced recombinant cell adhesion proteins Cys-axonin-1 and Cys-NgCAM retain their function after covalent immobilisation on glass and on gold. Neurite outgrowth from dissociated DRG neurons was observed and differences in the outgrowth promoting functions were reported.

- Measurement of the cell-surface distance with FLIC showed that the gap between the membrane and the electrode surface is at a minimum when axonin-1 is present.

- Patterning of proteins with photolithographic techniques showed that the proteins remained functional and promoted guided neurite outgrowth after patterning. Patterns of two proteins on one surface were created combining the etching and the lift-off method.

- Positioning of single neurons into the microgrooves was successful using a micromanipulator. However, the cells had moved out of the grooves after 24 h in culture.

- Neurons were cultured on functionalised microstructured chips and the electrical activity of the cells was confirmed by patch clamp recordings. Extracellular gold electrodes were used to stimulate single neurons while recording with an intracellular patch electrode.

6.2 Outlook

It can be concluded that the presented results are promising in view of future developments towards MEAs for stimulation and recording of single cells in a network. For the development of the electrode arrays several points have to be considered:

- Extracellular *recordings* with the existing neurochip will show, if the adhesion molecule present on the surface can improve the recorded signal. From the literature (see 4.4) it can be expected that, with a cell-surface distance of 40 nm, signals in the 1 mV range can be recorded.

- A new design of the chip can be proposed based on the experiences made: The dimensions of the groove hosting the cell should be adapted to the cell type. This can be done with test grooves of different dimensions in which the cells are placed with a micromanipulator. In order to allow connections between neurons to be made the grooves should be connected to each other via narrower channels for the neurites. Electrodes will then be situated under the cell body in the larger groove as well as in the channels for the neurites. With an appropriate surface coating of the channel ground (as discussed in 3.4) axon/dendrite polarity could be induced. Through the combination of topographic (channels) and chemical (surface coating) guidance a small network of 9–16 cells could be obtained.

- As already mentioned a few systems for in vivo neuron recording with MEAs are already on the market. An evaluation of these systems will show, if the present chip design (size and distribution of contact pads) has to be adapted to one of the existing recording systems. Alternatively, chip *and* periphery (hard- and software) has to be developed. Independent of this decision the chip size needs to be increased. With a side length of 2 cm, for example, the contact pads can be arranged along the edges of the chip. Pin arrays or zebra strips can then be used for contacting the chip. This would facilitate the chip handling during immobilisation, cell culturing and cleaning.

- The functionalisation of the chip surface with adhesion molecules offers a high flexibility. As mentioned above, axon/dendrite polarity could be induced by patterns of proteins on the surface. During the formation of the neural network, the presence of glia cells should be prevented. Glia cells preferently attach on RGDC rather than on NgCAM. Therefore, on the new neurochip a central area for adhesion of neurons, with patterns of NgCAM in the channels for the neurites surrounded by an area of RGDC, is proposed. If the above mentioned working hypothesis is confirmed by extracellular recording experiments, the electrodes will be functionalised with axonin-1 in order to achieve good signal transfer from the membrane to the electrode.

The functionalisation of surfaces with adhesion proteins is not only suitable for guiding neurite outgrowth. For applications in cell-based biosensors adhesion of other cell types in defined areas or in patterns is interesting. If a protein that promotes the attachment of a specific cell type is immobilised, the surface could be used to isolate one cell type from a cell suspension. Patterns of two or more such proteins on one surface could then be regarded as cell-sorter: A mixture of cells is plated on the surface and each cell type attaches only to the area with the specific protein. Such co-culture systems are interesting for applications in implant research, neuroscience and other fields.

Seite Leer /
Blank leaf

7

Abbreviations

APTES	Aminopropyltriethoxysilane
CAM	Cell adhesion molecule
CCD	Charge coupled device
DRG	Dorsal root ganglion
ECM	Extracellular matrix
FET	Field effect transistor
FITC	Fluorescein isothiocyanate
FLIC	Fluorescence interference contrast microscopy
FN	Fibronectin-type domain
FUdR	5-fluorodeoxyuridine/uridine
Ig	Immunoglobulin
IR-DIC	Infrared differential interference contrast microscopy
MBS	m-Maleimidobenzoyl-N-hydroxysulfosuccinimide ester
MEA	Multielectrode array
MEM	Minimal essential medium
MES	Mercaptoethanesulfonate
MPTMS	Mercaptopropyltrimethoxysilane
Ng-CAM	Neuron-glia cell adhesion molecule
NGF	Nerve growth factor
ODS	Octadecyltrichlorosilane
PBS	Phosphate buffered saline
PDMS	Polydimethylsiloxane
PEG-silane	O-[2-(Trimethyloxysilyl)ethyl]-O'-methyl-polyethylene glycol
RGDC	Arginine-glycine-aspartate-cysteine
rIgG	Rabbit-immunoglobulin G
S/N-ratio	Signal-to-noise ratio
sGMBS	N-[γ-Maleimidobutyryloxy]sulfosuccinimide ester

TBS   Tris buffered saline

TFS   Tridecafluoro-1,1,2,2-tetrahydrooctyl trichlorosilane

TRITC   Tetramethylrhodamine isothiocyanate

8

References

Albright, T. D., Jessell, T. M., Kandel, E. R., and Posner, M. I. 2000. Neural Science: A century of progress and the mysteries that remain. *Neuron* **25**: S1-S55.

Arregui, C. O., Carbonetto, S., and McKerracher, L. 1994. Characterization of neural cell adhesion sites: point contacts are the sites of interaction between integrins and the cytoskeleton in PC12 cells. *J. Neurosci.* **14**: 6967-6977.

Benson, D. L., Schnapp, L. M., Shapiro, L., and Huntley, G. W. 2000. Making memories stick: cell-adhesion molecules in synaptic plasticity. *Trends Cell Biol.* **10**: 473-482.

Blawas, A. S. and Reichert, W. M. 1998. Protein patterning. *Biomaterials* **19**: 595-609.

Bove, M., Grattarola, M., and Verreschi, G. 1997. *In vitro* 2-D networks of neurons characterized by processing the signals recorded with a planar microtransducer array. *IEEE Trans. Biomed. Eng.* **44**: 964-977.

Branch, D. W., Corey, J. M., Weyhenmeyer, J. A., Brewer, G. J., and Wheeler, B. C. 1998. Microstamp patterns of biomolecules for high-resolution neuronal networks. *Med. Biol. Eng. Comput.* **36**: 135-141.

Branch, D. W., Wheeler, B. C., Brewer, G. J., and Leckband, D. E. 2000. Long-term maintenance of patterns of hippocampal pyramidal cells on substrates of polyethylene glycol and microstamped polylysine. *IEEE Trans. Biomed. Eng.* **47**: 290-300.

Braun, D. and Fromherz, P. 1997. Fluorescence interference-contrast microscopy of cell adhesion on oxidized silicon. *Appl. Phys. A* **65**: 341-348.

Braun, D. and Fromherz, P. 1998. Fluorescence interferometry of neuronal cell adhesion on microstructured silicon. *Phys. Rev. Lett.* **81**: 5241-5244.

Breckenridge, L. J., Wilson, R. J. A., Connolly, P., Curtis, A. S. G., Dow, J. A. T., Blackshaw, S. E., and Wilkinson, C. D. W. 1995. Advantages of using microfabricated extracellular electrodes for *in vitro* neuronal recordings. *J. Neurosci. Res.* **42**: 266-276.

Britland, S., Perridge, C., Denyer, M., Morgan, H., Curtis, A. S. G., and Wilkinson, C. D. W. 1996. Morphogenic guidance cues can interact synergistically and hierarchically in steering nerve cell growth. *Exp. Biol. Online* **1**.

Brummendorf, T., Hubert, M., Treubert, U., Leuschner, R., Tarnok, A., and Rathjen, F. G. 1993. The axonal recognition molecule F11 is a multifunctional protein: specific domains mediate interactions with Ng-CAM and restrictin. *Neuron* **10**: 711-727.

Burridge, K. and Chrzanowska-Wodnicka, M. 1996. Focal adhesions, contractility, and signalling. *Annu. Rev. Cell Biol.* **12**: 463-519.

Chiu, D. T., Jeon, N. L., Huang, S., Kane, R. S., Wargo, C. J., Choi, I. S., Ingber, D. E., and Whitesides, G. M. 2000. Patterned deposition of cells and proteins onto surfaces by using three-dimensional microfluidic systems. *PNAS* **97**: 2408-2413.

Connolly, P., Clark, P., Curtis, A. S. G., Dow, J. A. T., and Wilkinson, C. D. W. 1990. An extracellular microelectrode array for monitoring electrogenic cells in culture. *Biosens. Bioelectron.* **5**: 223-234.

Curtis, A., Wilikinson, C. and Breckenridge, L.. 1994. Living nerve nets. *In* Enabling technologies for cultured neural networks. Stenger, D. A. and McKenna, T. M., editors. Academic Press Inc., San Diego. 99-120.

Curtis, A. S. G. and Wilkinson, C. D. W. 1997. Topographical control of cells. *Biomaterials* **18**: 1573-1583.

Davis, J. Q., McLaughlin, T., and Bennett, V. 1993. Ankyrin-binding proteins related to nervous system cell adhesion molecules: candidates to provide transmembrane and intercellular connections in adult brain. *J. Cell Biol.* **121**: 121-133.

Davis, J. Q. and Bennett, V. 1994. Ankyrin binding activity shared by the neurofascin/L1/NrCAM family of nervous system cell adhesion molecules. *J. Biol. Chem.* **269**: 27163-27166.

Dee, K. C., Rueger, D. C., Andersen, T. T., and Bizios, R. 1996. Conditions which promote mineralization at the bone-implant interface: a model *in vitro* study. *Biomaterials* **17**: 209-215.

Delamarche, E., Bernard, A., Schmid, H., Michel, B., and Biebuyck, H. 1997. Patterned delivery of immunoglobulins to surfaces using microfluidic networks. *Science* **276**: 779-781.

Denyer, M. C., Britland, S., Curtis, A. S. G., and Wilkinson, C. D. W. 1997. Patterned living neural networks on microfabricated microelectronic electrophysiological recording devices. *Cell. Eng.* **2**: 122-131.

Dichter, M. A. and Fischbach, G. D. 1977. The action potential of chick dorsal root ganglion neurones maintained in cell culture. *J. Physiol.* **267**: 281-298.

Duport, S., Millerin, C., Muller, D., and Corrèges, P. 1999. A metallic multisite system designed for continuous long-term monitoring of electrophysiological activity in slice cultures. *Biosens. Bioelectron.* **14**: 369-376.

Engel, J., Odermatt, E., Engel, A., Madri, J. A., Furthmayr, H., Rohde, H., and Timpl, R. 1981. Shapes, domain organizations and flexibility of laminin and fibronectin, two multifunctional proteins of the extracellular matrix. *J. Mol. Biol.* **150**: 97-120.

Esch, T., Lemmon, V., and Banker, G. 1999. Local presentation of substrate molecules directs axon specification by cultured hippocampal neurons. *J. Neurosci.* **19**: 6417-6426.

Felsenfeld, D. P., Hynes, M. A., Skoler, K. M., Furley, A. J., and Jessel, T. M. 1994. TAG-1 can mediate homophilic binding, but neurite outgrowth on TAG-1 requires an L1-like molecule and $\beta 1$ integrins. *Neuron* **12**: 675-690.

Fitzli, D., Stoeckli, E. T., Kunz, S., Siribour, K., Rader, C., Kunz, B., Kozlov, S. V., Buchstaller, A., Lane, R. P., Suter, D. M., Dreyer, W. J., and Sonderegger, P. 2000. A direct interaction of axonin-1 with NgCAM-related cell adhesion molecule (NrCAM) results in guidance, but not growth of commissural axons. *J. Cell Biol.* **149**: 951-968.

Flemming, R. G., Murphy, C. J., Abrams, G. A., Goodman, S. L., and Nealey, P. F. 1999. Effects of synthetic micro- and nano-structured surfaces on cell behaviour. *Biomaterials* **20**: 573-588.

Flounders, A. W., Brandon, D. L., and Bates, A. H. 1997. Patterning of immobilized antibody layers *via* photolithography and oxygen plasma exposure. *Biosens. Bioelectron.* **12**: 447-456.

Freigang, J., Proba, K., Leder, L., Diederichs, K., Sonderegger, P., and Welte, W. 2000. The crystal structure of the ligand binding molecule of axonin-1/TAG-1 suggests a zipper mechanism for neural cell adhesion. *Cell* **101**: 425-433.

Friedlander, D. R., Milev, P., Karthikeyan, L., Margolis, R. K., Margolis, R. U., and Grumet, M. 1994. The neuronal chondroitin sulfate proteoglycan neurocan binds to the neural cell adhesion molecules Ng-CAM/L1/NILE and N-CAM, and inhibits neuronal adhesion and neurite outgrowth. *J. Cell Biol.* **125**: 669-680.

Fromherz, P., Offenhäusser, A., Vetter, T., and Weis, J. 1991. A neuron-silicon junction: a retzius cell of the leech on an insulated-gate field-effect transistor. *Science* **252**: 1290-1293.

Fromherz, P. and Schaden, H. 1994. Defined neuronal arborizations by guided outgrowth of leech neurons in culture. *Eur. J. Neurosci.* **6**: 1500-1504.

Glass, J., Blevitt, J., Dickerson, K., Pierschbacher, M. D., and Craig, W. S. 1994. Cell attachment and motility on materials modified by surface-active RGD-containing peptides. *Annals New York Acad. Science (Biochemical engineering VIII)* **745**: 177-186.

Grattarola, M., Martinoia, S., Massobrio, G., Cambiaso, A., Rosichini, R., and Tetti, M. 1991. Computer simulations of the responses of passive and active integrated microbiosensors to cell activity. *Sensors Actuators B* **4**: 261-265.

Grattarola, M. and Martinoia, S. 1993. Modeling the neuron-microtransducer junction: from extracellular to patch recording. *IEEE Trans. Biomed. Eng.* **40**: 35-41.

Grattarola, M., Bove, M., Verreschi, G., and Giugliano, M. 1997. Signal analysis of simulated experiments: *in vitro* synchronised activity of networks of neurons coupled to arrays of planar microelectrodes. *Cell. Eng.* **2**: 154-160.

Grattarola, M. and Massobrio, G. 1998. Neurons and neuronal networks. *In* Bioelectronics Handbook: MOS-FETs, Biosensors, and Neurons. Grattarola, M. and Massobrio, G., editors. McGraw-Hill, 315-350.

Gross, G. W. and Schwalm, F. U. 1994. A closed flow chamber for long-term multichannel recording and optical monitoring. *J. Neurosci. Methods* **52**: 73-85.

Gross, G. W., Rhoades, B. K., Azzazy, H. M. E., and Wu, M. C. 1995. The use of neuronal networks on multielectrode arrays as biosensors. *Biosens. Bioelectron.* **10**: 553-567.

Gross, G. W., Norton, S., Gopal, K., Schiffmann, D., and Gramowski, A. 1997a. Neuronal networks *in vitro*: applications to neurotoxicology, drug development and biosensors. *Cell. Eng.* **2**: 138-147.

Gross, G. W., Harsch, A., Rhoades, B. K., and Göpel, W. 1997b. Odor, drug and toxin analysis with neuronal networks *in vitro*: extracellular array recording of network responses. *Biosens. Bioelectron.* **12/5**: 373-393.

Grumet, A. E., Wyatt Jr., J. L., and Rizzo III, J. F. 2000. Multi-electrode stimulation and recording in the isolated retina. *J. Neurosci. Methods* **101**: 31-42.

Grumet, M. and Edelman, G. M. 1988. Neuron-glia cell adhesion molecule interacts with neurons and astroglia via different binding mechanisms. *J. Cell Biol.* **106**: 487-503.

Grumet, M. 1991. Cell adhesion molecules and their subgroups. *Curr. Opin. Neurobiol.* **1**: 370-376.

Grumet, M., Mauro, V., Burgoon, M. P., Edelman, G. M., and Cunningham, B. A. 1991. Structure of a new nervous system glycoprotein, Nr-CAM, and its relationship to subgroups of neural cell adhesion molecules. *J. Cell Biol.* **113**: 1412.

Grumet, M., Friedlander, D. R., and Edelman, G. M. 1993. Evidence for the binding of Ng-CAM to laminin. *Cell Adhes. Commun.* **1**: 177-190.

Gundersen, R. W. 1985. Sensory neurite growth cone guidance by substrate adsorbed nerve growth factor. *J. Neurosci. Res.* **13**: 199-212.

Hammarback, J. A., Palm, S. L., Furcht, L. T., and Letourneau, P. C. 1985. Guidance of neurite outgrowth by pathways of substratum-absorbed laminin. *J. Neurosci. Res.* **13**: 213-220.

Harsch, A., Ziegler, C., and Göpel, W. 1997. Strychnine analysis with neuronal networks *in vitro*: extracellular array recording of network responses. *Biosens. Bioelectron.* **12**: 827-835.

Huber, M., Heiduschka, P., Kienle, S., Pavlidis, C., Mack, J., Walk, T., Jung, G., and Thanos, S. 1998. Modification of glassy carbon surfaces with synthetic laminin-derived peptides for nerve cell attachment and neurite growth. *J. Biomed. Mat. Res.* **41**: 278-288.

James, D. W. and Tresman, R. L. 1972. The surface coats of chick dorsal root ganglion cells *in vitro*. *J. Neurocytology* **1**: 383-395.

Jimbo, Y., Robinson, H. P. C., and Kawana, A. 1993. Simultaneous measurement of intracellular calcium and electrical activity from patterned neural networks in culture. *IEEE Trans. biomed. eng.* **40**: 804-810.

Kamioka, H., Maeda, E., Jimbo, Y., Robinson, H. P. C., and Kawana, A. 1996. Spontaneous periodic synchronized bursting during formation of mature patterns of connections in cortical cultures. *Neurosci. Lett.* **206**: 109-112.

Kamioka, H., Jimbo, Y., Charlety, P. J., and Kawana, A. 1997. Planar electrode arrays for long-term measurement of neuronal firing in cultured cortical slices. *Cell. Eng.* **2**: 148-153.

Kane, R. S., Takayama, S., Ostuni, E., Ingber, D. E., and Whitesides, G. M. 1999. Patterning proteins and cells using soft lithography. *Biomaterials* **20**: 2363-2376.

Klebe, R. J. 1988. Cytoscribing - a method for micropositioning cells and the construction of two dimensional and three dimensional synthetic tissues. *Exp. Cell Res.* **179**: 362-373.

Kleinfeld, D., Kahler, K. H., and Hockberger, P. E. 1988. Controlled outgrowth of dissociated neurons on patterned substrates. *J. Neurosci.* **8**: 4098-4120.

Kovacs, G. T. A. 1994. Introduction to the theory, design, and modeling of thin-film microelectrodes for neural interfaces. *In* Enabling technologies for cultured neural networks. Stenger, D. A. and McKenna, T. M., editors. Academic Press Inc., San Diego. 121-165.

Krnjevic, K. and Miledi, R. 1958. Motor units in the rat diaphragm. *J. Physiol.* **140**: 427-439.

Kuhn, T. B., Stoeckli, E. T., Condrau, M. A., Rathjen, F. G., and Sonderegger, P. 1991. Neurite outgrowth on immobilized axonin-1 is mediated by a heterophilic interaction with L1(G4). *J. Cell Biol.* **115**: 1113-1126.

Kunz, S., Ziegler, U., Kunz, B., and Sonderegger, P. 1996. Intracellular signaling is changed after clustering of the neural cell adhesion molecules axonin-1 and Ng-CAM during neurite fasciculation. *J. Cell Biol.* **135**: 253-267.

Kunz, S., Spirig, M., Ginsburg, C., Buchstaller, A., Berger, P., Lanz, R. B., Rader, C., Vogt, L., Kunz, B., and Sonderegger, P. 1998. Neurite fasciculation mediated by complexes of axonin-1 and Ng-cell adhesion molecule. *J. Cell Biol.* **143**: 1674-1690.

Lambacher, A. and Fromherz, P. 1996. Fluorescence interference-contrast microscopy on oxidized silicon using a monomolecular dye layer. *Appl. Phys. A* **63**: 207-216.

Letourneau, P. C. 1975. Cell-to-substratum adhesion and guidance of axonal elongation. *Develop. Biol.* **44**: 92-101.

Lierheimer, R., Kunz, B., Vogt, L., Savoca, R., Brodbeck, U., and Sonderegger, P. 1997. The neuronal cell-adhesion molecule axonin-1 is specifically released by an endogenous glycosylphosphatidylinositol-specific phospholipase. *Eur. J. Biochem.* **243**: 502-510.

Lind, R., Connolly, P., Wilkinson, C. D. W., and Thomson, R. D. 1991. Finite-element analysis applied to extracellular microelectrode design. *Sensors & Actuators B* **3**: 23-30.

Linss, W., Pilgrim, C., and Feuerstein, H. 1991. How thick is the glycocalyx of human erythrocytes? *Acta Histochem.* **91**: 101-104.

Lom, B., Healy, K. E., and Hockberger, P. E. 1993. A versatile technique for patterning biomolecules onto glass coverslips. *J. Neurosci. Methods* **50**: 385-397.

Lustig, M., Sakurai, T., and Grumet, M. 1999. Nr-CAM promotes neurite outgrowth from peripheral ganglia by a mechanism involving axonin-1 as a neuronal receptor. *Develop. Biol.* **209**: 340-351.

MacAlear, J. and Wehrung, J. 1978. Microsubstrates and method for making micropatternd devices. [4,103,073] US Patent.

Maeda, E., Robinson, H. P. C., and Kawana, A. 1995. The mechanisms of generation and propagation of synchronized bursting in developing networks of cortical neurons. *J. Neurosci.* **15**: 6834-6845.

Maher, M. P., Pine, J., Wright, J., and Tai, Y.-C. 1999. The neurochip: a new multielectrode device for stimulating and recording from cultured neurons. *J. Neurosci. Methods* **87**: 45-56.

Martinoia, S., Bove, M., Tedesco, M., Margesin, B., and Grattarola, M. 1999. A simple microfluidic system for patterning populations of neurons on silicon micromachined substrates. *J. Neurosci. Methods* **87**: 34-44.

Massia, S. P. and Hubbell, J. A. 1990. Covalent surface immobilization of Arg-Gly-Asp- and Tyr-Ile-Gly-Ser-Arg-containing peptides to obtain well-defined cell-adhesive substrates. *Anal. Biochem.* **187**: 292-301.

Matsuzawa, M., Liesi, P., and Knoll, W. 1996. Chemically modifying glass surfaces to study substratum-guided neurite outgrowth in culture. *J. Neurosci. Methods* **69**: 189-196.

Matsuzawa, M., Umemura, K., Beyer, D., Sugioka, K., and Knoll, W. 1997. Micropatterning of neurons using organic substrates in culture. *Thin solid films* **305**: 74-79.

McKeehan, W. L. and Ham, R. G. 1976. Stimulation of clonal growth of normal fibroblasts with substrata coated with basic polymers. *J. Cell Biol.* **71**: 727-734.

McKerracher, L., Chamoux, M., and Arregui, C. O. 1996. Role of laminin and integrin interactions in growth cone guidance. *Mol. Neurobiol.* **12**: 95-116.

Milev, P., Friedlander, D. R., Sakurai, T., Karthikeyan, L., Flad, M., Margolis, R. K., Grumet, M., and Margolis, R. U. 1994. Interactions of the chondroitin sulfate proteoglycan phosphacan, the extracellular domain of a receptor-type protein tyrosine phosphatase with neurons, glia, and neural cell adhesion molecules. *J. Cell Biol.* **127**: 1703-1715.

Milev, P., Maurel, P., Haring, M., Margolis, R. K., and Margolis, R. U. 1996. TAG-1/axonin-1 is a high-affinity ligand of neurocan, phosphacan/protein-tyrosine phosphatase Zeta/Beta, and N-CAM. *J. Biol. Chem.* **271**: 15716-15723.

Montgomery, A. M. P., Becker, J. C., Siu, C. H., Lemmon, V. P., Cheresh, D. A., Pancook, J. D., Zhao, X. N., and Reisfeld, R. A. 1996. Human neural cell adhesion molecule L1 and rat homologue NILE are ligands for integrin $\alpha_v\beta_3$. *J. Cell Biol.* **132**: 475-485.

Moscoso, L. M. and Sanes, J. R. 1995. Expression of four immunoglobulin superfamily adhesion molecules (L1, NrCAM/Bravo, neurofascin/AGBP, and N-CAM) in the developing mouse spinal cord. *J. Comp. Neurol.* **352**: 321-334.

Mrksich, M. and Whitesides, G. M. 1995. Patterning self-assembled monolayers using microcontact printing: A new technology for biosensors? *Trends Biotechnol.* **13**: 228-235.

Müller, T., Gradl, G., Howitz, S., Shirley, S., Schnelle, Th., and Fuhr, G. 1999. A 3-D microelectrode system for handling and caging single cells and particles. *Biosens. Bioelectron.* **14**: 247-256.

Nermut, M. V., Green, N. M., Eason, P., Yamada, S. S., and Yamada, K. M. 1988. Electron microscopy and structural model of human fibronectin receptor. *EMBO J.* **7**: 4093-4099.

Nicolau, D. C., Taguchi, T., Taniguchi, H., Tanigawa, H., and Yoshikawa, S. 1999. Patterning neuronal and glia cells on light-assisted functionalised photoresists. *Biosens. Bioelectron.* **14**: 317-325.

Offenhäusser, A., Sprössler, C., Matsuzawa, M., and Knoll, W. 1997. Field-effect transistor array for monitoring electrical activity from mammalian neurons in culture. *Biosens. Bioelectron.* **12**: 819-826.

Oka, H., Shimono, K., Ogawa, R., Sugihara, H., and Taketani, M. 1999. A new planar multielectrode array for extracellular recording: application to hippocampal acute slice. *J. Neurosci. Methods* **93**: 61-67.

Padeste, C., Grubelnik, A., and Tiefenauer, L. 2000. Ferrocene-avidin conjugates for bioelectrochemical applications. *Biosens. Bioelectron.* **15**: 431-438.

Pancrazio, J. J., Bey Jr.P.P., Loloee, A., Manne, S., Chao, H., Howard, L. L., Gosney, W. M., Borkholder, D. A., Kovacs, G. T. A., Manos, P., Cuttino, D. S., and Stenger, D. A. 1998. Description and demonstration of a CMOS amplifier-based-system with measurement and stimulation capability for bioelectrical signal transduction. *Biosens. Bioelectron.* **13**: 971-979.

Pompe, T., Fery, A., Herminghaus, S., Kriele, A., Lorenz, H., and Kotthaus, J. P. 1999. Submicron contact printing on silicon using stamp pads. *Langmuir* **15**: 2398-2401.

Rader, C., Stoeckli, E. T., Ziegler, U., Osterwalder, T., Kunz, B., and Sonderegger, P. 1993. Cell-cell adhesion by homophilic interaction of the neuronal recognition molecule axonin-1. *Eur. J. Biochem.* **215**: 133-141.

Rader, C., Kunz, B., Lierheimer, R., Giger, R. J., Berger, Ph., Tittmann, P., Gross, H., and Sonderegger, P. 1996. Implications for the domain arrangement of axonin-1 derived from the mapping of its NgCAM binding site. *EMBO J.* **15**: 2056-2068.

Rathjen, F. G. and Jessell, M. 1991. Glycoproteins that regulate the growth and guidance of vertebrate axons: domains and dynamics of the immunoglobulin/fibronectin type III subfamily. *Semin. Neurosci.* **3**: 297-307.

Regehr, W. G., Pine, J., and Rutledge, D. B. 1988. A long-term *in vitro* silicon-based microelectrode-neuron connection. *IEEE Trans. Biomed. Eng.* **35**: 1023-1032.

Regehr, W. G., Pine, J., Cohan, C. S., Mischke, M. D., and Tank, D. W. 1989. Sealing cultured invertebrate neurons to embedded dish electrodes facilitates long-term stimulation and recording. *J. Neurosci. Methods* **30**: 91-106.

Reichhardt, L. F. and Tomaselli, K. J. 1991. Extracellular matrix molecules and their receptors: functions in neural development. *Annu. Rev. Neurosci.* **14**: 531-570.

Ruegg, M. A., Stoeckli, E. T., Lanz, R. B., Streit, P., and Sonderegger, P. 1989. A homologue of the axonally secreted protein axonin-1 is an integral membrane protein of nerve fiber tracts involved in neurite fasciculation. *J. Cell Biol.* **109**: 2363-2378.

Ruppert, M., Aigner, S., Hubbe, M., Yagita, H., and Altevogt, P. 1995. The L1 adhesion molecule is a cellular ligand for VLA-5. *J. Cell Biol.* **131**: 1881-1891.

Schiffer, M., Girling, R. L., Ely, K. R., and Edmundson, A. B. 1973. Structure of a lambda-type Bence-Jones protein at 3.5-Å resolution. *Biochemistry* **12**: 4620-4631.

Schmitt, G., Schultze, J. W., Fassbender, F., Buss, G., Lüth, H., and Schöning, M. J. 1999. Passivation and corrosion of microelectrode arrays. *Electrochimica Acta* **44**: 3865-3883.

Sigrist, H., Collioud, A., Clémence, J. F., Gao, H., Luginbühl, R., Sänger, M., and Sundarababu, G. N. 1995. Surface immobilization of biomolecules by light. *Optical Engineering* **34/8**: 2339-2348.

Sonderegger, P., Lemkin, P. F., Lipkin, L. E., and Nelson, P. G. 1985. Differentiation modulation of the expression of axonal proteins by non-neuronal cells of the peripheral and central nervous system. *EMBO J.* **4**: 1395-1401.

Sonderegger, P. and Rathjen, F. G. 1992. Regulation of axonal growth in the vertebrate nervous system by interactions between glycoproteins belonging to two subgroups of the immunolglobulin superfamily. *J. Cell Biol.* **119**: 1387-1394.

Sonderegger, P. 1998. Ig superfamily molecules in the nervous system. Harwood academic publishers, Amsterdam NL.

Sorribas, H., Braun, D., Leder, L., Sonderegger, P., and Tiefenauer, L. 2001. Adhesion proteins for a tight neuron-electrode contact. *J. Neurosci. Methods* **104**: 133-141.

Stenger, D. A., Georger, J. H., Dulcey, C. S., Hickman, J. J., Rudolph, A. S., Nielsen, T. B., McCort, S. M., and Calvert, J. M. 1992. Coplanar molecular assemblies of amino- and perfluorinated alkylsilanes: characterization and geometric definition of mammalian cell adhesion and growth. *J. Am. Chem. Soc.* **114**: 8435-8442.

Stenger, D. A., Hickman, J. J., Bateman, K. E., Ravenscroft, M. S., Ma, W., Pancrazio, J. J., Shaffer, K., Schaffner, A. E., Cribbs, D. H., and Cotman, C. W. 1998. Microlithographic determination of axonal/dendritic polarity in cultured hippocampal neurons. *J. Neurosci. Methods* **82**: 167-173.

Stoeckli, E. T., Kuhn, T. B., Duc, C. O., Ruegg, M. A., and Sonderegger, P. 1991. The axonally secreted protein axonin-1 is a potent substratum for neurite growth. *J. Cell Biol.* **112/3**: 449-455.

Stoeckli, E. T. and Landmesser, L. T. 1995. Axonin-1, Nr-CAM, and Ng-CAM play different roles in the *in vivo* guidance of chick commissural neurons. *Neuron* **14**: 1165-1179.

Stoeckli, E. T., Ziegler, U., Bleiker, A. J., Groscurth, P., and Sonderegger, P. 1996. Clustering and functional cooperation of Ng-CAM and axonin-1 in the substratum-contact area of growth cones. *Develop. Biol.* **177**: 15-29.

Stoeckli, E. T., Sonderegger, P., Pollerberg, G. E., and Landmesser, L. T. 1997. Interference with axonin-1 and NrCAM interactions unmask a floor-plate activity inhibitory for commissural axons. *Neuron* **18**: 209-221.

Streeter, H. B. and Rees, D. A. 1987. Fibroblast adhesion to RGDS shows novel features compared with fibronectin. *J. Cell Biol.* **105**: 507-515.

Suter, D. M., Pollerberg, E. G., Buchstaller, A., Giger, R. J., Dreyer, W. J., and Sonderegger, P. 1995. Binding between the neural cell adhesion molecules axonin-1 and Nr-CAM/Bravo is involved in neuron-glia interaction. *J. Cell Biol.* **131**: 1067-1081.

Svoboda, K. and Block, S. M. 1994. Biological applications of optical forces. *Annu. Rev. Biophys. Biomol. Struct.* **23**: 247-285.

Takeda, Y., Asou, H., Murakami, Y., Miura, M., Kobayashi, M., and Uyemura, K. 1996. A nonneuronal isoform of cell adhesion molecule L1: tissue-specific expression and functional analysis. *J. Neurochem.* **66**: 2338-2349.

Takeichi, M. 1991. Cadherin cell adhesion receptors as a morphogenetic regulator. *Science* **251**: 1451-1455.

Tawil, N., Wilson, P., and Carbonetto, S. 1993. Integrins in point contacts mediate cell spreading: factors that regulate integrin accumulation in point contacts vs. focal contacts. *J. Cell Biol.* **120**: 261-271.

Tessier-Lavigne, M. and Goodman, C. S. 1996. The molecular biology of axon guidance. *Science* **274**: 1123-1133.

Townes-Anderson, E., St.Jules, R. S., Sherry, D. M., Lichtenberger, J., and Hassanain, M. 1998. Micromanipulation of retinal neurons by optical tweezers. *Molecular Vision* **4**: 12-17.

Vaidya, R., Tender, L. M., Bradley, G., O'Brien II, M. J., Cone, M., and López, G. P. 1998. Computer-controlled laser ablation: a convenient and versatile tool for micropatterning biofunctional synthetic surfaces for applications in biosensing and tissue engineering. *Biotechnol. Prog.* **14**: 371-377.

Vassanelli, S. and Fromherz, P. 1999. Transistor probes local potassium conductances in the region of cultured rat hippocampal neurons. *J. Neurosci.* **19**: 6767-6773.

Vielmetter, J., Stolze, B., Bonhoeffer, F., and Stuermer, C. A. O. 1990. In vitro assay to test differential substrate affinities of growing axons and migratory cells. *Exp. Brain Res.* **8**: 283-287.

Weiss, P. 1945. Experiments on cell and axon orientation in vitro: the role of colloidal exudates in tissue organization. *J. Exp. Zool.* **100**: 353-386.

Wilkinson, C. D. W. and Curtis, A. S. G. 1999. Networks of living cells. *Physics World* **12**: 45-48.

Wilson, R. J. A., Breckenridge, L., Blackshaw, S. E., Connolly, P., Dow, J. A. T., Curtis, A. S. G., and Wilkinson, C. D. W. 1994. Simultaneous multisite recordings and stimulation of single isolated leech neurons using planar extracellular electrode arrays. *J. Neurosci. Methods* **53**: 101-110.

Wojciak-Stothard, B., Curtis, A., Monaghan, W., Macdonald, K., and Wilkinson, C. D. W. 1996. Guidance and activation of murine macrophages by nanometric scale topography. *Exp. Cell Res.* **223**: 426-435.

Yavin, E. and Yavin, Z. 1974. Attachment and culture of dissociated cells from rat embryo cerebral hemispheres on polylysine-coated surface. *J. Cell Biol.* **62**: 540-546.

Yoshihara, Y., Kawasaki, M., Tamada, A., Nagata, S., Kagamyiama, H., and Mori, K. 1995. Overlapping and differential expression of BIG-2, BIG-1, TAG-1 and F3: four members of an axon-associated cell adhesion molecule subgroup of the immunoglobulin family. *J. Neurobiol.* **28**: 51-69.

List of publications

Reviewed papers:

Vuilleumier, S., Sorribas, H., and Leisinger, T. 1997. Identification of a novel determinant of glutathione affinity in dichloromethane dehalogenases/glutathione S-transferases. *Biochem. Biophys. Res. Commun.* **238**(2):452-456.

Sorribas, H., Padeste, C., Mezzacasa, T, Tiefenauer, L., Leder, L., Fitzli, D., and Sonderegger, P. 1999. Neurite outgrowth on microstructured surfaces functionalized by a neural adhesion protein. *J.Mat.Science: Materials Medicine* **10**: 787-791.

Sorribas, H., Braun, D., Leder, L., Sonderegger, P., and Tiefenauer, L. 2001. Adhesion proteins for a tight neuron-electrode contact. *J. Neurosci. Methods* **104**: 133-141.

Sorribas, H., Padeste, C., and Tiefenauer, L. 2001. Photolithographic generation of protein patterns. *Submitted to Biomaterials*.

Conferences/Abstracts:

Sorribas, H., Padeste, C., Gennser, U., Sonderegger, P., and Tiefenauer, L. Microstructured biofunctionalised glass for neuron cell guidance and recording. *Biosensors 1998*, Berlin (D).

Sorribas, H., Leder, L., Fitzli, D., Padeste, C., Mezzacasa, T., Sonderegger, P., and Tiefenauer, L. Neurite outgrowth on microstructured surfaces functionalized by a neural adhesion protein. *15th Conference of the European Society for Biomaterials 1999*, Arcachon (F).

Sorribas, H., Leder, L., Padeste, C., Sonderegger, P., and Tiefenauer, L. Patterns of the adhesion protein axonin-1 for neurite guidance on glass. *Axon Guidance and Neural Plasticity*, EMBO Workshop 1999, Varenna (I).

Sorribas, H., Leder, L., Padeste, C., Sonderegger, P., and Tiefenauer, L. Patterning adhesion proteins for neuron guidance on glass. *USGEB 1999*, Basel (CH).

Sorribas, H., Padeste, C., Sonderegger, P., and Tiefenauer, L. Patterns of adhesion molecules for cell guidance. *Swiss Society of Biomaterials SSB 6th annual meeting 2000*, Davos (CH).

Sorribas, H., Braun, D., Padeste, C., Sonderegger, P., and Tiefenauer, L. Neurite Outgrowth on surfaces treated with neural cell adhesion molecules. *2nd Multi-electrode array MEA Meeting 2000*, Naturwissenschaftliches und Medizinisches Institut, Universität Tübingen (D).

Curriculum vitae

Name	Helga Maria Sorribas
Date of birth	January 12, 1973
Citizenship	Spain

Education

1987-1992	Gymnasium Typus D, Chur
1992-1997	Biology at the Swiss Federal Institute of Technology in Zürich
	Diploma subjects: Biochemistry, Molecular Biology and Biophysics, Principles of Microbiology, Immunology, Genetics
	Diploma thesis: Protein Engineering Untersuchungen zur Gluta-thion-Affinität von Dichlormethan-Dehalogenasen/Glutathion S-Transferasen. Performed at the Institute of Microbiology ETHZ (Prof. Th. Leisinger)
1997-2001	PhD at the Laboratory for Micro- and Nanotechnology, Paul Scherrer Institut (Villigen) in collaboration with Prof. R. J. Douglas at the Institute of Neuroinformatics, Uni/ETHZ

Seite Leer /
Blank leaf

Acknowledgements

Seite Leer /
Blank leaf